Universität Bonn

Forschungszentrum Jülich

Exploring topological structure of graphene nanoribbons with Hubbard interactions

Lado Razmadze

BCS-Hubbard model is applied to nanoribbons with zigzag and armchair geometries. Dispersion relations and effective Hamiltonian are derived at symmetric lines for ferromagnetic and antiferromagnetic order. Conserved quantities are found for general case of BCS-Hubbard model.

Forschungszentrum Jülich
Wilhelm-Johnen-Straße
52428 Jülich

BONN-IR-2021-XXX
Dez 2021

Universität Bonn

Forschungszentrum Jülich

Exploring topological structure of graphene nanoribbons with Hubbard interactions

Lado Razmadze

Dieser Forschungsbericht wurde als Masterarbeit von der
Mathematisch-Naturwissenschaftlichen Fakultät der Universität Bonn angenommen.

Angenommen am:	11.12.2021
1. Gutachter:	Prof. Dr. Thomas Luu
2. Gutachter:	Prof. Dr. Ulf G. Meißner

Acknowledgements

I would like to thank Dr. Thomas Luu who offered to be my supervisor and gave me a fantastic opportunity of working with him at Forschungszentrum Jülich on my master's thesis. He was always available for quick questions as well as interesting and insightful discussions that were very valuable during my research.

I would also like to thank Dr. Akaki Rusetsky for his continued support and help. He is the reason why I decided to get my master's degree at University of Bonn and was always available to answer any and all questions throughout my studies.

Contents

CHAPTER 1

Introduction

Study of materials has been a human endeavor from the discovery of flint knapping. Ever since first people discovered that certain rocks like flint cleave very cleanly and leave an incredibly thin edge began a materials' arms race. Then came the age of metal which brought new materials and techniques for example smelting and alloying. Ancient civilizations, like Greeks, were the first to think about the why of it all. Lucretius cleverly reasoned that since destruction takes much less effort and time than creation, through wear and tear everything would eventually turn into nothing. Therefore, there must be something small and indivisible (atomos) that makes up everything and prevents the eternal decay. Dalton built on ideas like these to explain why this newfangled science called chemistry was even possible by creating a prototype of the periodic table of elements, which was later perfected by Mendeleev. Later still Linus Pauling used the up-and-coming field of quantum mechanics to explain chemical bonds and earned himself a Nobel prize in chemistry. The idea of using quantum mechanics turned out to be very fruitful as it led to the discovery of superconductivity and superfluidity. Today the bleeding edge of research involves 1D and 2D materials like graphene nanotubes, nanoribbons and sheets. Newest methods by which we study these things are based on mathematics of group theory and topology

CHAPTER 2

Quantum Description of Matter

In this section most of the information is taken from [1], [2], [3], [4]

2.1 Quantum Primer

Describing a quantum system requires only a single *wave function* - $\Psi(\mathbf{x}, t)$, where t is time and $\mathbf{x}$ is a vector containing all possible *degrees of freedom*(DOF) like space, spin etc. Usually spatial DOFs - $\mathbf{r}$ are separated from the rest of the *quantum numbers* - σ and the wave function is written as $\Psi_\sigma(\mathbf{r}, t)$. Wave function contains all the information about system dynamics, which is described by a well known *Schrödinger Eq.*

$$i\hbar\partial_t \Psi_\sigma(\mathbf{r}, t) = \mathrm{H}\Psi_\sigma(\mathbf{r}, t) \tag{2.1}$$

H is the Hamiltonian that defines the system under consideration. Using Fourier technique for solving linear partial differential equations(PDEs) wave function is written as

$$\Psi_\sigma(\mathbf{r}, t) = \int \frac{\mathrm{d}E}{2\pi\hbar}\, e^{-iEt/\hbar}\, \tilde{\Psi}_\sigma(\mathbf{r}, E) \tag{2.2}$$

Depending on H and the boundary conditions, energy - E may take on discrete values E_n(which usually is the case). So we rewrite (2.1) and finally arrive at the desired time-independent Schrödinger eq.

$$\mathrm{H}\tilde{\Psi}_{n\sigma}(\mathbf{r}) = E_{n\sigma}\tilde{\Psi}_{n\sigma}(\mathbf{r}) \tag{2.3}$$

After solving this *eigenvalue* equation we will have complete description of the system, with *eigenvectors* spanning *Hilbert space* - $\mathcal{H}$. If the energy difference between the lowest excited state and the ground state remains finite as we take the size of the system to be infinite (thermodynamic limit), we say that system is *gapped*. Interestingly the question of whether or not a system is gapped is undecidable[5], but that is not a issue for the problems we encounter on a daily basis. Gapped systems play an important role in topological condensed matter as we will see in the following chapters.

2.2 Crystals and Lattices

Materials like flint, diamond, graphene or even plain table salt are known as *crystalline*, since they are composed of a regular arrangement of atoms called *lattices*. It may not seem like it but metals are also made up of lattices, however, one often forgets about internal regularity of metals since they can be fashioned into almost any macroscopic shape. Unfortunately for us when it comes to many body systems like these (2.3) quickly becomes intractable, so in order to study the behavior of such systems we need to make simplifications. For lattices one of the most useful approximations is called *tight-binding* which, along with the symmetries that a given lattice may possess, greatly simplify mathematical description and enable us to study them in depth.

In physics a lattice, more specifically a *Bravais lattice* is a translationally invariant system of identical subsystems or *bases*, also known as *primitive unit cells*. These can be atoms, molecules, etc. that are separated by distances of the order a - called a *lattice constant*. We formalize this by defining a set of basis vectors $\{\mathbf{a}_i\}_{i=1\ldots d}$, where d is the dimension of the lattice and arbitrary translation vector $\mathbf{R}_n = \sum_i n_i \mathbf{a}_i$ with $n_i \in \mathbb{Z}$. If the bases placed at lattice cites are not point-like then we have to define additional vectors $\{\tau_\alpha\}_{\alpha=1\ldots n}$ to describe their inner structure. Now the notion of translational invariance can be written as

$$\mathrm{H}(\mathbf{r} + \mathbf{R}_n) = \mathrm{H}(\mathbf{r}) \tag{2.4}$$

meaning the translation vector takes the lattice and maps it to itself. As an example consider graphene (fig. 2.1), which is a sheet of carbon atoms arranged in hexagonal pattern. It is described as a triangular lattice spanned by $\mathbf{a}_{1,2} = (3/2, \pm\sqrt{3}/2)$(shown in purple) with two atoms in each unit cell. Another way of looking at it is to imagine two identical triangular sublattices shifted with respect to each other. Green arrows point to *nearest neighbors* on sublattice A In this figure they are $\tau_1 = (-1, 0)$,

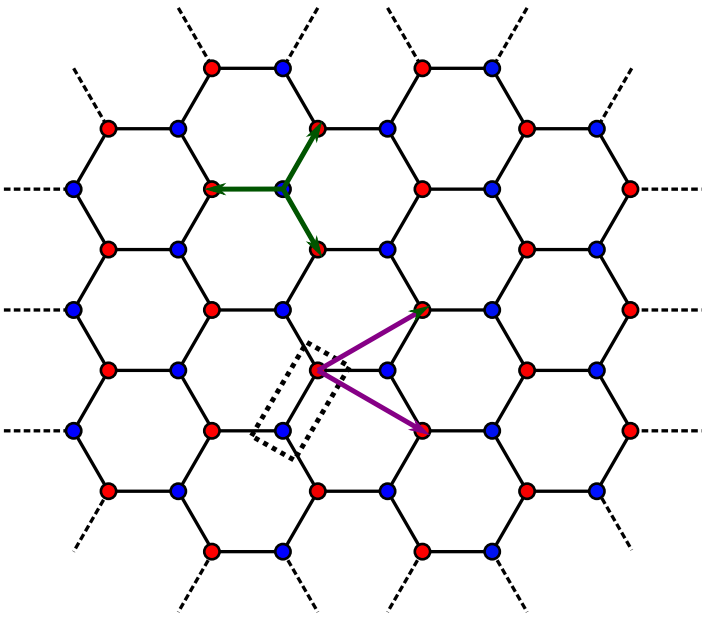

Figure 2.1: Graphene lattice. Unit cell in dashed rectangle. Sublattice A is in blue while sublattice B in red. Nearest neighbor vectors are in green and next nearest in purple.

$\tau_2 = (1/2, \sqrt{3}/2)$ and $\tau_3 = (1/2, -\sqrt{3}/2)$. Note that nearest neighbor vectors have opposite signs on sublattices A and B.

2.3 Bloch's Theorem

To be mathematically rigorous one could say the lattice is invariant under *d-dimensional translation group* - $\mathbb{Z}^d$. More often than not lattices have higher level of symmetry but we will only consider translations for now. This assumption already allows for mathematical simplification summarized by *Bloch's theorem* named after *Felix Bloch*[6]. Bloch's theorem is a concrete realization of a more general *Floquet's theorem* applied to Schrödinger equation. Simply put it states that a periodic Hamiltonian will yield periodic solutions with a phase factor. To prove aforementioned theorem we define translation operator $T(\mathbf{R})$ on the Hilbert space of functions as

$$T(\mathbf{R})\Psi(\mathbf{r}) = \Psi(\mathbf{r}+\mathbf{R}) \tag{2.5}$$

$T(\mathbf{R})$ is a representation of $\mathbb{Z}^d$

$$T^{-1}(\mathbf{R})\Psi(\mathbf{r}+\mathbf{R}) = \Psi(\mathbf{r}) = \Psi(\mathbf{r}+\mathbf{R}-\mathbf{R}) = T(-\mathbf{R})\Psi(\mathbf{r}+\mathbf{R}) \tag{2.6}$$

$$T(\mathbf{R}_2)T(\mathbf{R}_1)\Psi(\mathbf{r}) = \Psi(\mathbf{r}+\mathbf{R}_1+\mathbf{R}_2) = T(\mathbf{R}_1+\mathbf{R}_2)\Psi(\mathbf{r}) \tag{2.7}$$

Since Hamiltonian is translationally invariant it commutes with $T(\mathbf{R})$

$$T(\mathbf{R})H(\mathbf{r})\Psi(\mathbf{r}) = \mathrm{H}(\mathbf{r}+\mathbf{R})\Psi(\mathbf{r}+\mathbf{R}) = \mathrm{H}(\mathbf{r})T(\mathbf{R})\Psi(\mathbf{r})$$

meaning that they are simultaneously diagonalizable. Assuming $\Psi(\mathbf{r})$ is an eigenstate of these operators we can write

$$T(\mathbf{R})\Psi(\mathbf{r}) = \lambda(\mathbf{R})\Psi(\mathbf{r}) \tag{2.8}$$

From the properties of T's we can conclude

$$\lambda(\mathbf{R_1}+\mathbf{R_2}) = \lambda(\mathbf{R_1})\lambda(\mathbf{R_2}) \tag{2.9}$$

Using normalization condition we impose additional restriction on $\lambda(\mathbf{R})$. Translated wave function is still normalized to 1 so we can write

$$1 = |T(\mathbf{R})\Psi(\mathbf{R})| = |\lambda(\mathbf{R})||\Psi(\mathbf{R})| = |\lambda(\mathbf{R})| \tag{2.10}$$

This multiplicative functional equation has a simple solution

$$\lambda(\mathbf{R}) = e^{i\mathbf{k}\cdot\mathbf{R}} \tag{2.11}$$

with

$$\mathbf{k} = \sum_i x_i \mathbf{b}_i \tag{2.12}$$

such that $\mathbf{b}_i \cdot \mathbf{a}_j = 2\pi\delta_{ij}$.

$$T(\mathbf{R})\Psi(\mathbf{r}) = e^{i\mathbf{k}\cdot\mathbf{R}}\Psi(\mathbf{r}) \tag{2.13}$$

This result can be reproduced using group theory (see A). That approach is generalizable beyond translation to more complicated point symmetries in addition to the symmetries of the orbitals placed inside the crystals. It was first used by Bethe [7] and it became a foundation of what is now known as *topological band theory*.

2.4 Band Theory

For the Schrödinger eq. to be a *well posed* differential equation we need to define *boundary conditions*. Main assumption here is that for a lattice with $\sim O(N)$ cites, surface to bulk ratio of particles is $\sim O(N^{-(d-1)/d})$ where d is the dimension, and since $N \sim O(10^{23})$ we assume boundary effects to be negligible and choose ones that simplify calculation. One such boundary condition would be to assume that the lattice extent(measured in lattice cites) in i'th direction is L_i and define *Born-von Karman* periodic boundary conditions as

$$\forall\, i, \quad \Psi(\mathbf{r} + L_i \mathbf{a}_i) = \Psi(\mathbf{r}) \tag{2.14}$$

Using the results from previous section we can deduce

$$\Psi(\mathbf{r}) = \Psi(\mathbf{r} + L_i \mathbf{a}_i) = e^{i\mathbf{k}\cdot\mathbf{a}_i L_i}\Psi(\mathbf{r}) \tag{2.15}$$

furthermore

$$e^{i\mathbf{k}\cdot\mathbf{a}_i L_i} = e^{i\sum_j x_j \mathbf{b}_j \cdot \mathbf{a}_i L_i} = e^{i x_i 2\pi L_i} = 1 \tag{2.16}$$

meaning

$$x_i = \frac{m_i}{L_i}, \qquad m_i \in \mathbb{Z} \tag{2.17}$$

Which results in the wave vector quantization

$$\mathbf{k} = \sum_i \frac{m_i}{L_i}\mathbf{b}_i \tag{2.18}$$

This result allows us to rewrite the wave function without loss of generality (WLOG) as

$$\Psi(\mathbf{r}) = e^{i\mathbf{k}\cdot\mathbf{r}} u_{\mathbf{k}}(\mathbf{r}) \tag{2.19}$$

$$u_{\mathbf{k}}(\mathbf{r}) = u_{\mathbf{k}}(\mathbf{r} + \mathbf{R}) \tag{2.20}$$

The set $\{\mathbf{b}_i\}_{i=1\ldots d}$ is known as *reciprocal lattice basis* and it spans the reciprocal lattice space (also known as momentum space). Smallest unit cell in this space is called a *first Brillouin zone* (1BZ). For example a 1-dimensional 1BZ is the range

$$1BZ = \left(-\frac{\pi}{a}, \frac{\pi}{a}\right) \tag{2.21}$$

Now every energy eigenvalue depends on $\mathbf{k}$, so we can scan reciprocal lattice space and plot the locus of varying energy levels. These loci are called *energy bands*. One can learn a lot by just looking at the band structure of the system.

2.5 Tight-Binding Approximation

If the atom at one of the lattice cites is described by Hamiltonian H_{at}, then WLOG we write

$$\mathrm{H}_{\text{lattice}} = \mathrm{H}_{\text{at}} + \Delta U(\mathbf{r}) \tag{2.22}$$

where $\Delta U(\mathbf{r})$ contains information about the potential of the rest of the lattice. For simplicity we assume only one electron that is to say only one kinetic term. This will be generalized to multi-particle case in the next section.

The name tight-binding is self-explanatory, in this formalism we assume atomic(or subsystem) wave functions to be localized around lattice cites, that is to say, their wave functions decay rapidly at the distances of order a, and treat the overlap between neighboring cites as a perturbation. This way we are able to use the eigenfunctions $\phi_n(\mathbf{r})$ of individual cites to construct the solutions $\Psi_{n\mathbf{k}}(\mathbf{r})$ of the whole crystal. Assuming individual atoms obey

$$\mathrm{H}_{\text{at}}\phi_n(\mathbf{r}) = E_n\phi_n(\mathbf{r}) \tag{2.23}$$

while

$$\mathrm{H}_{\text{lattice}}\Psi_{n\mathbf{k}}(\mathbf{r}) = E_n(\mathbf{k})\Psi_{n\mathbf{k}}(\mathbf{r}) \tag{2.24}$$

Even in the simple case of graphene we have a lattice with two cites per base. We can't just use a simple direct product of atomic wave functions since it won't posses the symmetries discussed in section 2.3. Fortunately only a small modification is need approximate the crystal wave function. For each sublattice write

$$\Phi_{m\alpha\mathbf{k}}(\mathbf{r}) = \frac{1}{\sqrt{N}}\sum_{\mathbf{R}_\alpha} e^{i\mathbf{k}\cdot\mathbf{R}_\alpha}\phi_m(\mathbf{r}-\mathbf{R}_\alpha) \tag{2.25}$$

where $\mathbf{R}_\alpha$ are the points the α'th sublattice and ϕ_m is the It can easily be checked that this linear combination obeys Bloch's theorem

$$\begin{aligned}\Phi_{m\alpha\mathbf{k}}(\mathbf{r}+\mathbf{R}'_\alpha) &= \frac{1}{\sqrt{N}}\sum_{\mathbf{R}_\alpha} e^{i\mathbf{k}\cdot\mathbf{R}_\alpha}\phi_m(\mathbf{r}-\mathbf{R}_\alpha+\mathbf{R}'_\alpha) &(2.26)\\ &= e^{i\mathbf{k}\cdot\mathbf{R}'_\alpha}\frac{1}{\sqrt{N}}\sum_{\mathbf{R}_\alpha} e^{i\mathbf{k}\cdot(\mathbf{R}_\alpha-\mathbf{R}'_\alpha)}\phi_m(\mathbf{r}-(\mathbf{R}_\alpha-\mathbf{R}'_\alpha)) &(2.27)\\ &= e^{i\mathbf{k}\cdot\mathbf{R}}\Phi_{m\alpha\mathbf{k}}(\mathbf{r}) &(2.28)\end{aligned}$$

Crystal wave function can be given as a superposition of sublattices

$$\Psi_{n\mathbf{k}}(\mathbf{r}) = \sum_{m\alpha} c_{nm\alpha}(\mathbf{k})\Phi_{m\alpha\mathbf{k}}(\mathbf{r}) \tag{2.29}$$

Coefficients $c_{nm\alpha}(\mathbf{k})$ can be found using *variational method*. Since the energy of this state is given by

$$E_n(\mathbf{k}) = \frac{\langle\Psi_{n\mathbf{k}}|H_{\text{lattice}}|\Psi_{n\mathbf{k}}\rangle}{\langle\Psi_{n\mathbf{k}}|\Psi_{n\mathbf{k}}\rangle} = \frac{\sum_{mm'\alpha\beta} c^*_{nm\alpha}(\mathbf{k})c_{nm'\beta}(\mathbf{k})H_{m\alpha,m'\beta}}{\sum_{mm'\alpha\beta} c^*_{nm\alpha}(\mathbf{k})c_{nm'\beta}(\mathbf{k})S_{m\alpha,m'\beta}} \tag{2.30}$$

with

$$H_{m\alpha,m'\beta} = \langle \Phi_{m\alpha\mathbf{k}}(\mathbf{r}) | H_{\text{lattice}} | \Phi_{m'\beta\mathbf{k}}(\mathbf{r}) \rangle \tag{2.31}$$

$$S_{m\alpha,m'\beta} = \langle \Phi_{m\alpha\mathbf{k}}(\mathbf{r}) | \Phi_{m'\beta\mathbf{k}}(\mathbf{r}) \rangle \tag{2.32}$$

we demand that the derivative w.r.t. $c_{nm\alpha}(\mathbf{k})$ (alternatively $c^*_{nm\alpha}(\mathbf{k})$) vanish, this leads us to

$$\sum_{m'\beta} (H_{m\alpha,m'\beta} - E_n(\mathbf{k}) S_{m\alpha,m'\beta}) c_{nm'\beta} = 0 \tag{2.33}$$

For this system of equations to have non-trivial solutions the matrix has to be singular.

$$\det(H_{m\alpha,m'\beta} - E_n(\mathbf{k}) S_{m\alpha,m'\beta}) = 0 \tag{2.34}$$

We can calculate energy levels for graphene. First we note that here only p_z orbitals contribute, meaning we can drop the m and m' indices. Moreover we only have two sublattices A and B, so the equation simplifies to

$$\det \begin{pmatrix} H_{AA} - E_n(\mathbf{k}) S_{AA} & H_{AB} - E_n(\mathbf{k}) S_{AB} \\ H_{BA} - E_n(\mathbf{k}) S_{BA} & H_{BB} - E_n(\mathbf{k}) S_{BB} \end{pmatrix} = 0 \tag{2.35}$$

We can go through this term-by-term (see B)

$$H_{AA} = \sum_{\mathbf{d}} e^{i\mathbf{k}\cdot\mathbf{d}} \langle \phi(\mathbf{r}) | H_{\text{lattice}} | \phi(\mathbf{r} - \mathbf{d}) \rangle \tag{2.36}$$

Here we only keep the nearest neighbor terms. Now $\langle \phi(\mathbf{r}) | H_{\text{lattice}} | \phi(\mathbf{r}) \rangle \equiv \epsilon_{p_z}$ is the energy of orbital p_z. Rest of terms in this series contribute next nearest terms. Similar calculation is done for H_{BB} which leads to

$$H_{AA} = H_{BB} = \epsilon_{p_z} \tag{2.37}$$

Next

$$H_{AB} = \sum_{\mathbf{d}} e^{i\mathbf{k}\cdot\mathbf{d}} \langle \phi(\mathbf{r}) | H_{\text{lattice}} | \phi(\mathbf{r} - \mathbf{d}) \rangle \tag{2.38}$$

Again we only consider term up to nearest neighbors denoted by $\langle nn \rangle$. Due to the symmetry of Hamiltonian $\langle \phi(\mathbf{r}) | H_{\text{lattice}} | \phi(\mathbf{r} - \mathbf{d}) \rangle \equiv t$ is the same for all $\mathbf{d} \in \langle nn \rangle$. Let

$$f(\mathbf{k}) = \sum_{\mathbf{d} \in \langle nn \rangle} e^{i\mathbf{k}\cdot\mathbf{d}} \tag{2.39}$$

and we get

$$H_{AB} = H^*_{BA} = f(\mathbf{k}) t \tag{2.40}$$

Similar calculations for $S_{\alpha\beta}$ gives

$$S_{AA} = S_{BB} = 1 \tag{2.41}$$

$$S_{AB} = S^*_{BA} = s f(\mathbf{k}) \tag{2.42}$$

Using this we get

$$\det\begin{pmatrix} \epsilon_{p_z} - E_n(\mathbf{k}) & f(\mathbf{k})(t - E_n(\mathbf{k})s) \\ f(\mathbf{k})^*(t - E_n(\mathbf{k})s) & \epsilon_{p_z} - E_n(\mathbf{k}) \end{pmatrix} = 0 \tag{2.43}$$

Assuming sufficiently small s final result is

$$E_n(\mathbf{k}) - \epsilon_{p_z} = \pm t|f(\mathbf{k})| \tag{2.44}$$

2.6 Second Quantization

In order to describe the systems with more than one particle, we employ a technique called *second quantization* also known as *occupation number representation*. Instead of the Hilbert space $\mathcal{H}$ we deal with *Fock space* which is a direct product of Hilbert spaces of individual particles.

$$\mathcal{F} = \otimes_j \mathcal{H}_j \tag{2.45}$$

In case of fermions we have to consider *indistinguishability* and anti-symmetry under the exchange of two identical fermions. If $|\psi_1\rangle \in \mathcal{H}_1$ and $|\psi_2\rangle \in \mathcal{H}_2$ then an anti-symmetrized wave function would have the form

$$|\phi\rangle = |\psi_1\rangle \wedge |\psi_2\rangle \equiv \frac{1}{2}(|\psi_1\rangle \otimes |\psi_2\rangle - |\psi_2\rangle \otimes |\psi_1\rangle) \tag{2.46}$$

$\wedge$ is know as a wedge(antisymmetric) product. Fock space is given by anti-symmetrized tensor product also known as *outer product*

$$\mathcal{F} = \bigwedge_j \mathcal{H}_j \tag{2.47}$$

Since we are dealing solely with electrons we usually drop wedges and implicitly assume the anti-symmetric property to hold. Next we introduce *creation/annihilation* operators $c_j^\dagger / c_j$ for state j. Index j is a multi-index it may refer to location, spin polarization, angular momentum(orbital) etc. Now we can express complicated neighbor hopping and interactions in a very succinct way. Particle hopping from lattice cite j to l can be written as $-tc_l^\dagger c_j$, a particle is annihilated at j and created at l. A simple Hamiltonian for graphene with only nearest neighbor hopping looks like

$$H = -\mu \sum_l c^\dagger_{A\mathbf{r}_l} c_{A\mathbf{r}_l} + c^\dagger_{B\mathbf{r}_l} c_{B\mathbf{r}_l} - t \sum_{\langle i,j \rangle} c^\dagger_{A\mathbf{r}_i} c_{B\mathbf{r}_j} + h.c. \tag{2.48}$$

Here $\langle i, j \rangle$ means the sum is only over nearest neighbors. Hermitian conjugate $h.c.$ is added to account for the hopping in both directions. We can Fourier transform the operators as follows

$$c_{\lambda\mathbf{r}_j} = \frac{1}{\sqrt{N}} \sum_{\mathbf{k}} e^{i\mathbf{k}\cdot\mathbf{r}_j} c_{\lambda\mathbf{k}} \tag{2.49}$$

Inserting this into the hopping part of the Hamiltonian gives

$$H = -t\frac{1}{N} \sum_{\langle i,j \rangle \mathbf{k}\mathbf{k}'} e^{i\mathbf{k}\cdot\mathbf{r}_j - i\mathbf{k}'\cdot\mathbf{r}_i} c^\dagger_{A\mathbf{k}'} c_{B\mathbf{k}} + h.c. \tag{2.50}$$

$$= -t\frac{1}{N}\sum_{\langle i,j\rangle \mathbf{k}\mathbf{k}'} e^{i(\mathbf{k}-\mathbf{k}')\cdot\mathbf{r}_j - i\mathbf{k}'\cdot(\mathbf{r}_i-\mathbf{r}_j)} c^{\dagger}_{A\mathbf{k}'} c_{B\mathbf{k}} + h.c. \tag{2.51}$$

$$= -t\sum_{\mathbf{k}} f(\mathbf{k}) c^{\dagger}_{A\mathbf{k}} c_{B\mathbf{k}} + h.c. \tag{2.52}$$

Here we used the identity

$$\delta_{k',k} = \frac{1}{N}\sum_{j} e^{i(\mathbf{k}-\mathbf{k}')\cdot\mathbf{r}_j} \tag{2.53}$$

When we do similar calculations for the rest of the Hamiltonian, we arrive at

$$H = -\sum_{\mathbf{k}} \begin{pmatrix} c^{\dagger}_{A\mathbf{k}} & c^{\dagger}_{B\mathbf{k}} \end{pmatrix} \begin{pmatrix} \mu & f(\mathbf{k}) \\ f^*(\mathbf{k}) & \mu \end{pmatrix} \begin{pmatrix} c_{A\mathbf{k}} \\ c_{B\mathbf{k}} \end{pmatrix} \tag{2.54}$$

From the Hamiltonian final energies are derived to be

$$E(k) - \mu = \pm t|f(\mathbf{k})| \tag{2.55}$$

Result is the same as in the previous section and it took far less effort.

CHAPTER 3

Topology in condensed systems

Large part of this section is taken from [8], [9], [10], [11], [12].

3.1 Overview

Use of topological methods in condensed matter is relatively new and it was prompted by an experimental discovery of *Quantum Hall effect*(QHE) [13] by Klitzing et al. When a conductor is placed in strong magnetic field of order $\sim 15T$ and cooled down to the temperature $1.5K$ one observes the sample become gapped (insulating) in the bulk while the surface still remains conductive. Simple explanation of this phenomenon is that magnetic field causes electrons in the bulk to be trapped in the cyclotron orbits making the bulk insulating, however the cyclotron orbits can't close on the surface of the sample causing them to skip along the edges making them conductive (see fig. 3.1). Such a phenomenon can never be observed in regular insulators, which caused physicists to refine existing classification of matter. This extension is done by introducing *topological equivalence* on

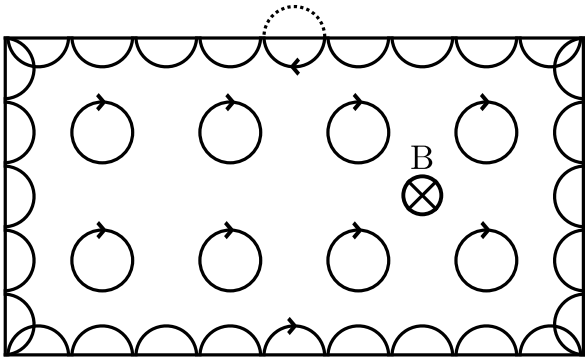

Figure 3.1: Quantum hall effect. Cyclotron orbits cause bulk to become insulating, but since they can't close on the edges electrons can skip along making them conductive.

the space of gapped hamiltonians. Key concept in topology is *continuity*. Two topological spaces are considered to be equivalent if they can be continuously mapped to each-other. Consider a space Ω of Hamiltonians. Two Hamiltonians are defined as topologically equivalent if the two can be

connected in the Hamiltonian space without closing the energy gap. Physically this corresponds to adiabatically changing the parameters to transform one Hamiltonian into another while every intermediate Hamiltonian remains gapped. In fig. 3.2 H and H'' are equivalent since there exists a path connecting them while satisfying this requirement. But H' is separated from H and H'' by a wall of gap closing denoted in red, meaning H and H' are topologically inequivalent. Having defined

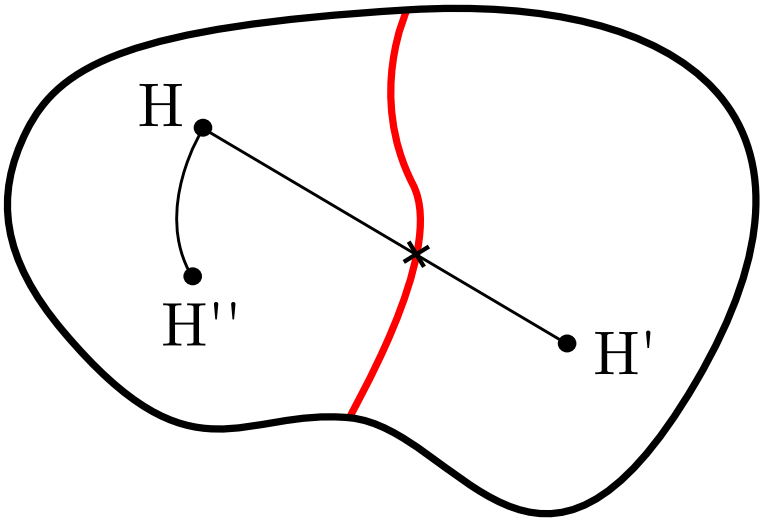

Figure 3.2: Hamiltonian space with two phases separated by wall of gap closing denoted in red. H and H'' are equivalent while H and H' are not.

equivalence we have to define a *topologically trivial phase*. For this we choose *atomic insulators* which are insulating because electrons are tightly bound to the atomic cores inside the solid. If a system is not topologically equivalent to an atomic insulator then we say that it is topological.

3.2 Kitaev chain

As an example of topological condensed matter system a Kitaev chain toy model is often used [11]. Kitaev introduced this system in order to argue that Majorana states could be created in solid state systems. His main motivation was development of Majoranas as qubits for quantum computing due to their robustness, which stems from the topological invariant that the system possesses - Parity. As a consequence this model exemplifies the world of topological matter very well.

The chain is a 1D system with nearest neighbor hopping t, nearest neighbor superconductive pairing Δ and chemical potential μ. These physical properties span our parameter space.

$$\mathrm{H} = -t\sum_{j=1}^{L-1}(c_j^\dagger c_{j+1} + h.c.) + \Delta\sum_{j=1}^{L-1}(c_j c_{j+1} + h.c.) - \mu\sum_{j=1}^{L} c_j^\dagger c_j \tag{3.1}$$

From introductory quantum mechanics we know that number operator is defined as $n_j = c_j^\dagger c_j$. We will be using these to interchangeably. First two sums don't include last lattice site due to open boundary

conditions. Additionally we know for both Bosonic and Fermionic operators

$$n_j|0\rangle_j = c_j^\dagger c_j|0\rangle_j = 0$$
$$n_j|1\rangle_j = c_j^\dagger c_j|1\rangle_j = |1\rangle_j$$

In order to solve this system we change to Majorana representation

$$c_j = \frac{1}{2}(\gamma_{ja} + i\gamma_{jb}), \qquad c_j^\dagger = \frac{1}{2}(\gamma_{ja} - i\gamma_{jb}) \tag{3.2}$$

Ordinary fermion operators c are *nilpotent* meaning $\exists n \in \mathbb{N} : c^n = 0$. For spin-1/2 particles like we have here, $n = 2$. Majorana fermions γ are superpositions of creation and annihilation operators of ordinary fermions, because of that they are no longer nilpotent, instead $\gamma^2 = 1$. They do, however, still retain the anti-commutation property of ordinary fermions, that is to say $\{\gamma_{i\lambda}, \gamma_{j\lambda'}\} = \delta_{ij}\delta_{\lambda\lambda'}$. Using these properties we can go through calculation term-by-term

$$\begin{aligned} c_j^\dagger c_{j+1} + h.c. &= \frac{1}{4}(\gamma_{ja} - i\gamma_{jb})(\gamma_{j+1a} + i\gamma_{j+1b}) + h.c. \\ &= \frac{1}{2}(i\gamma_{ja}\gamma_{j+1b} - i\gamma_{jb}\gamma_{j+1a}) \end{aligned}$$

Terms of the form $i\gamma_i\gamma_j$ are Hermitian and $\gamma_i\gamma_j$ skew-Hermitian so when we add h.c. former term doubles, whereas the latter vanishes. Similarly

$$\begin{aligned} c_j c_{j+1} + h.c. &= \frac{1}{4}(\gamma_{ja} + i\gamma_{jb})(\gamma_{j+1a} + i\gamma_{j+1b}) + h.c. \\ &= \frac{1}{2}(i\gamma_{ja}\gamma_{j+1b} + i\gamma_{jb}\gamma_{j+1a}) \end{aligned}$$

and

$$\begin{aligned} n_j = c_j^\dagger c_j &= \frac{1}{4}(\gamma_{ja} - i\gamma_{jb})(\gamma_{ja} + i\gamma_{jb}) \\ &= \frac{1}{2}(1 + i\gamma_{ja}\gamma_{jb}) \end{aligned}$$

Note that $i\gamma_{ja}\gamma_{jb} = (2n_j - 1)$ meaning

$$-i\gamma_{ja}\gamma_{jb}|0\rangle_j = |0\rangle_j \tag{3.3}$$
$$-i\gamma_{ja}\gamma_{jb}|1\rangle_j = -|1\rangle_j \tag{3.4}$$

So $-i\gamma_{ja}\gamma_{jb}$ is measures parity of j-th lattice site. Total parity operator can be constructed by taking products of these operators

$$P = \prod_{j=1}^{L}(-i\gamma_{ja}\gamma_{jb}) \tag{3.5}$$

Putting it all together gives

$$\mathrm{H} = \frac{-t+\Delta}{2}\sum_{j=1}^{L-1} i\gamma_{ja}\gamma_{j+1b} + \frac{t+\Delta}{2}\sum_{j=1}^{L-1} i\gamma_{jb}\gamma_{j+1a} - \frac{\mu}{2}\sum_{j=1}^{L}(1+i\gamma_{ja}\gamma_{jb}) \tag{3.6}$$

To show that this system has different phases first consider the case $t = \Delta = 0$ and $\mu > 0$. Hamiltonian reduces to

$$\mathrm{H}_0 = -\frac{\mu}{2}\sum_{j=1}^{L}(1+i\gamma_{ja}\gamma_{jb}) \tag{3.7}$$

with the ground state

$$|gs\rangle = \otimes_{j=1}^{L}|0\rangle_j \tag{3.8}$$

Now consider the case $t = \Delta, \mu = 0$, where we are left with

$$\mathrm{H}_1 = t\sum_{j=1}^{L-1} i\gamma_{jb}\gamma_{j+1a} \tag{3.9}$$

Since $(i\gamma_{jb}\gamma_{j+1a})^2 = 1$ ground state of H_1 would need to satisfy

$$i\gamma_{jb}\gamma_{j+1a}|gs\rangle^d = \pm|gs\rangle^d$$

To make sure that a ground state minimizes energy we choose:

$$-i\gamma_{jb}\gamma_{j+1a}|gs\rangle^d = |gs\rangle^d \tag{3.10}$$

Analogously to the c-fermions we define d-fermions, which are bound states of neighboring Majorana fermions.

$$d_j = \frac{1}{2}(\gamma_{jb} + i\gamma_{j+1a}), \qquad d_j^\dagger = \frac{1}{2}(\gamma_{jb} - i\gamma_{j+1a}) \tag{3.11}$$

After which Hamiltonian becomes

$$\mathrm{H}_1 = t\sum_{j=1}^{L-1}(2d_j^\dagger d_j - 1) \tag{3.12}$$

Define d-vacuum at cite j as $|0\rangle_j^d$ with obvious properties

$$d_j|0\rangle_j^d = 0 \qquad d_j^\dagger|0\rangle_j^d = |1\rangle_j^d \tag{3.13}$$

It becomes clear that ground state for this Hamiltonian is

$$|gs\rangle^d = \otimes_{j=1}^{L-1}|0\rangle_j^d \tag{3.14}$$

Since the sum only goes up to $L-1$ there is no $d_L^\dagger,\ d_L$ terms in Hamiltonian, implying the existence of *zero modes*, or excitations with zero energy. In this case the ground state is two-fold degenerate,

and the states are known as Majorana Zero modes(MZM).

$$\begin{aligned} \mathrm{H}_1|gs\rangle^d &= E|gs\rangle^d \\ \mathrm{H}_1(d_L^\dagger|gs\rangle^d) &= d_L^\dagger H_1|gs\rangle^d = E(d_L^\dagger|gs\rangle^d) \end{aligned}$$

We can distinguish these states by parity P. Parity operation on $|gs\rangle^d$ can be simplified using (3.10) and anti-commutativity of Majorana fermions.

$$\begin{aligned} P|gs\rangle^d = \prod_{j=1}^{L}(-i\gamma_{ja}\gamma_{jb})|gs\rangle^d &= (-i\gamma_{1a}\gamma_{1b})(-i\gamma_{2a}\gamma_{2b})\cdots(-i\gamma_{La}\gamma_{Lb})|gs\rangle^d \\ &= -(-i\gamma_{Lb}\gamma_{1a})(-i\gamma_{1b}\gamma_{2a})\cdots(-i\gamma_{L-1b}\gamma_{La})|gs\rangle^d \\ &= -|gs\rangle^d \end{aligned}$$

Whereas

$$P(d_L^\dagger|gs\rangle^d) = \prod_{j=1}^{L}(-i\gamma_{ja}\gamma_{jb})d_L^\dagger|gs\rangle^d = -d_L^\dagger\prod_{j=1}^{L}(-i\gamma_{ja}\gamma_{jb})|gs\rangle^d = d_L^\dagger|gs\rangle^d \tag{3.15}$$

So we can introduce new notation

$$\begin{aligned} |gs\rangle^d &= |-\rangle \\ d_L^\dagger|gs\rangle^d &= |+\rangle \end{aligned}$$

Ground state in this phase is doubly degenerate due to parity. As we can see for two sets of (t, Δ, μ) we get two Hamiltonians with different eigensystems. If we were to smoothly vary these parameters $(0, 0, \mu) \to (t, t, 0)$ there would be gap closing at $(t, t, 2t)$ which, from the definition in section 3, means that these two Hamiltonians represent topologically distinct phases. In general the $t = \Delta$ is known as *symmetric lines condition* and in this case it makes analytic solution of the problem possible.

3.3 Bogoliubov de Gennes (BdG) Hamiltonian

Sometimes in the study of condensed matter systems we encounter *quasi-particles* that are collective excitations of particles and holes. Majorana particles introduced in previous section are one example of such excitations. They are somewhat simple considering that the collective nature of Majoranas is localized to individual lattice cites.

Most notable method of describing such systems is *Bogoliubov transformation* which defines a new set of operators $\{b_i\}$ as a linear superposition of old ones $\{c_i\}$

$$b_i = u_{ij}c_j + v_{ij}c_j^\dagger \tag{3.16}$$

where u and v are c-numbers. Requiring that this transformation be *canonical*, meaning new operators must satisfy the same commutation/anticommutation relations as the old ones, we get a condition

$$u_{ik}u_{kj}^* + v_{ik}v_{kj}^* = \delta_{ij} \tag{3.17}$$

In order to introduce BdG in our system we rewrite (3.1) using *Nambu spinors* (see [14])

$$C_j = \begin{pmatrix} c_j \\ c_j^\dagger \end{pmatrix} \tag{3.18}$$

First write out the terms in Hamiltonian

$$\mathrm{H} = -\frac{t}{2}\sum_{j=1}^{L-1} c_j^\dagger c_{j+1} + c_{j+1}^\dagger c_j - c_{j+1}c_j^\dagger - c_j c_{j+1}^\dagger \tag{3.19}$$

$$+\frac{\Delta}{2}\sum_{j=1}^{L-1} c_j c_{j+1} + c_{j+1}^\dagger c_j^\dagger - c_{j+1}c_j - c_j^\dagger c_{j+1}^\dagger \tag{3.20}$$

$$-\frac{\mu}{2}\sum_{j=1}^{L} c_j^\dagger c_j - c_j c_j^\dagger \tag{3.21}$$

We wrote down duplicate terms to make Hamiltonian symmetric. Now we can bring this equation to a matrix form

$$\mathrm{H} = \frac{1}{2}\sum_{j=1}^{L-1} C_j^\dagger \begin{pmatrix} -t & -\Delta \\ \Delta & t \end{pmatrix} C_{j+1} + \frac{1}{2}\sum_{j=1}^{L-1} C_{j+1}^\dagger \begin{pmatrix} -t & \Delta \\ -\Delta & t \end{pmatrix} C_j + \frac{1}{2}\sum_{j=1}^{L} C_j^\dagger \begin{pmatrix} -\mu & 0 \\ 0 & \mu \end{pmatrix} C_j \tag{3.22}$$

Introduce $C = (C_1, \cdots C_N)$, hopping operator $|i\rangle\langle j|$ from state j to state i, as well as Pauli matrices $\tau_{x,y,z}$ in Nambu spinor basis

$$\tau_x = \begin{pmatrix} 0 & 1 \\ 1 & 0 \end{pmatrix} \qquad \tau_y = \begin{pmatrix} 0 & -i \\ i & 0 \end{pmatrix} \qquad \tau_z = \begin{pmatrix} 1 & 0 \\ 0 & -1 \end{pmatrix} \tag{3.23}$$

Using these rewrite Hamiltonian into more manageable form

$$\mathrm{H} = \frac{1}{2} C^\dagger \mathrm{H}_{\mathrm{BdG}} C \tag{3.24}$$

with

$$\mathrm{H}_{\mathrm{BdG}} = -\sum_{j=1}^{L} \mu\tau_z \otimes |j\rangle\langle j| - \sum_{j=1}^{L-1} (t\tau_z + i\Delta\tau_y) \otimes |j\rangle\langle j+1| + h.c. \tag{3.25}$$

In order to reproduce the results from section 3.2 we set $t = \Delta$ and use a computer to solve for the energy levels of this Hamiltonian while varying μ with respect to(w.r.t.) t. That will lead us to fig. 3.3. We can clearly see zero modes that exist for a wide range of values of μ, as well as the transition at around $\mu = 2t$. It should be noted that Kitaev chain Hamiltonian at the symmetric lines is mathematically identical to another condensed matter system exhibiting topological properties - Su-Schrieffer-Heeger model of Polyaceylene [15].

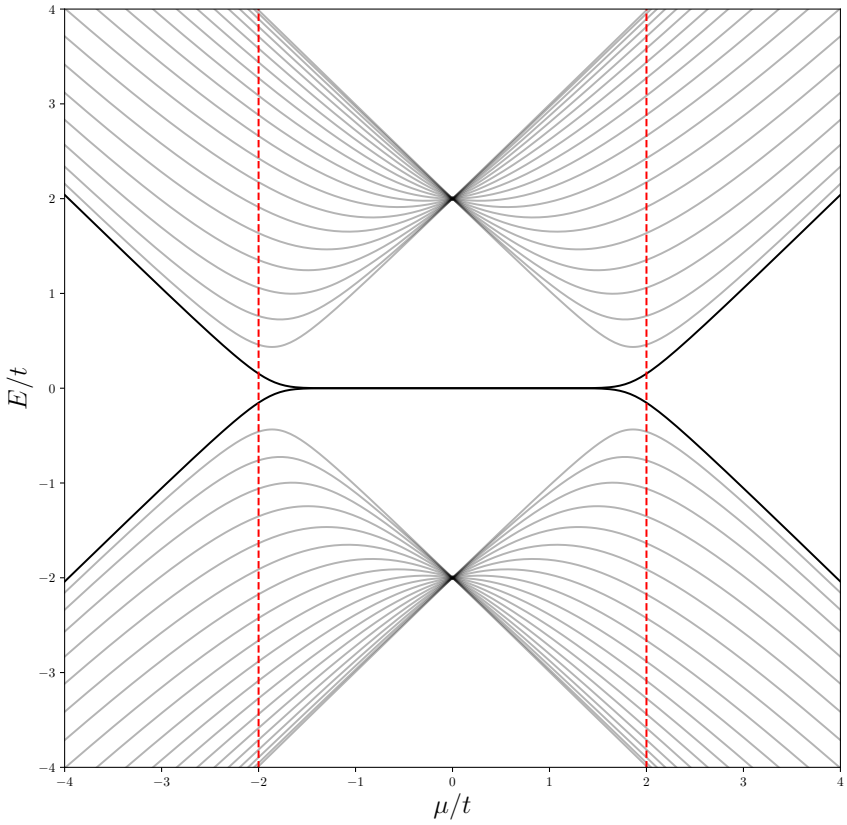

Figure 3.3: Energy level dependence on μ. Zero modes in solid black and $\mu = \pm 2t$ in dashed red

3.4 Momentum space

Continuing analysis from the previous section we introduce *Fourier transform*. One may argue that we can't use it here since it has an implicit assumption that edge effects are negligible, which is correct for large crystals but if we have only a handful of lattice cites we cannot neglect the effects that they introduce. For now assume that we are dealing with sufficiently large lattices so that we can disregard edge cites.

$$|j\rangle = \frac{1}{\sqrt{L}} \sum_k e^{-ikaj} |k\rangle \tag{3.26}$$

Inserting this in (3.1) and using

$$\sum_j e^{i(k-k')aj} = L\delta_{kk'} \tag{3.27}$$

we arrive at

$$\mathrm{H}_{\mathrm{BdG}} = -\sum_k \left(\mu\tau_z + (t\tau_z + i\Delta\tau_y)e^{ika} + (t\tau_z - i\Delta\tau_y)e^{-ika} \right) \otimes |k\rangle\langle k| \tag{3.28}$$

Which is a block-diagonal matrix with blocks of the form

$$\mathbf{d}(k) \cdot \boldsymbol{\tau} = -(\mu + 2t\cos(ka))\tau_z + 2\Delta\sin(ka)\tau_y \tag{3.29}$$

Eigenvalues can be easily derived as $E_k = \pm|\mathbf{d}(k)|$

$$E_k = \pm\sqrt{(\mu + 2t\cos(ka))^2 + 4\Delta^2\sin^2(ka)} \tag{3.30}$$

If we plot this at symmetric lines for various μ/t we observe that there is a gap closing around $k = 0$ for $\mu = -2t$ and around $k = \pm\pi$ for $\mu = 2t$, see fig. 3.5. We write the *effective field Hamiltonian* by Taylor expanding $\mathbf{d}(k)$ around $k = \pi$ to the first order in ka

$$\mathbf{d}(k) \approx -(\mu - 2t)\tau_z - 2\Delta ka\tau_y \tag{3.31}$$

This is a called *Dirac Hamiltonian* in one dimension since it is linear in momentum. The mass term $m = \mu - 2t$ vanishes for $\mu = 2t$ and we end up with a dispersion relation of massless particles.

$$E_k \propto \pm v|k| \tag{3.32}$$

$\pm v$ implies that we have two massless modes moving in opposite directions see fig. 3.4.

Figure 3.4: left/right moving massless modes on a Kitaev chain

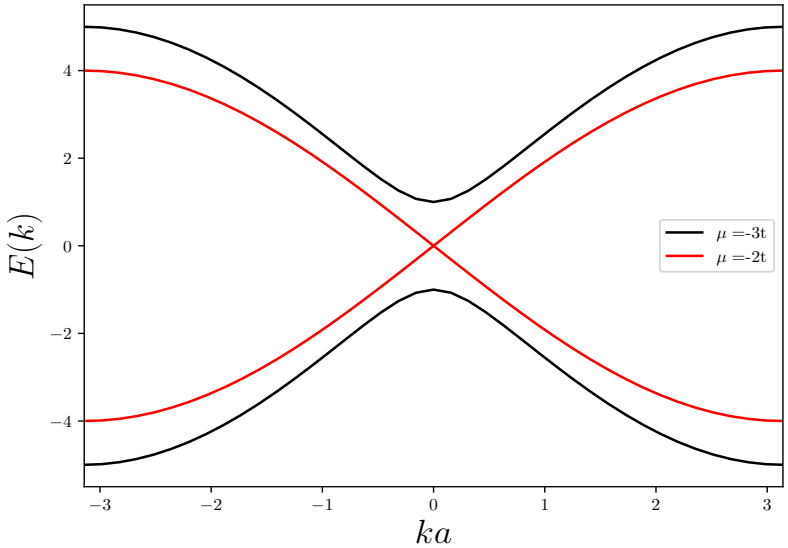

Figure 3.5: Energy levels for various μ. Note gap closing at 0 and at $\pm\pi$ for $\mu = -2t$ and $\mu = 2t$ respectively

3.5 Bulk edge correspondence

One of the qualities of topological phases is non-locality, namely correlation between states on the edge of the system and in the bulk, hence the term bulk edge correspondence. In a sense edge states have information about the whole system. This is exemplified by Kitaev chain model. We saw that in the $(t, t, 0)$ phase we had two fold degeneracy due to Majorana zero modes. Looking closer we see that the culprit was $d_L = (\gamma_{Lb} + i\gamma_{1a})/2$. This operator creates a state that is not localized anywhere and instead is split between the endpoints of our 1D lattice. This is why MZM are also called the edge modes.

It must be noted that edge modes are very robust. As we have seen in section 3.4 for symmetric lines Kitaev chain can be described using massless Dirac Hamiltonian, which gives rise to left/right moving chiral states. That is not a specific to the Kitaev chain Hamiltonian though. We can take many such chains and stack them together. As long as there is a coupling between modes of opposite chirality between neighboring chains we will still end up with topological phase with edge modes along the top and bottom of the stack see fig. 3.6. Bulk edge correspondence is inherent to these topological phases, however exispence of edge modes is not sufficient to tell wether the state is topological or not.

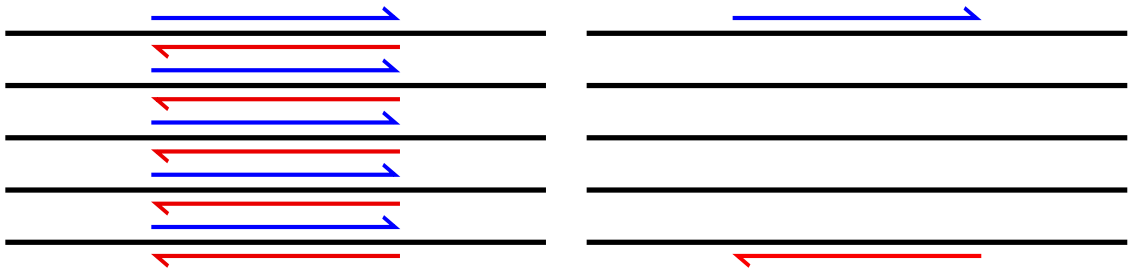

(a) Stacked kitaev chains

(b) Effective edge modes

Figure 3.6: By stacking kitaev chains at $\mu = 2t$ we observe 1D edge modes after the left/right moving modes cancel each other out in the bulk.

CHAPTER 4

BCS-Hubbard Model on a Bipartite Lattice

This section will heavily borrow from [16], [17] and [18].

4.1 Hamiltonian

Consider an N-dimensional general bipartite lattice with nearest neighbor hopping - t and superconductive(SC) pairing - Δ. Hopping and SC are defined only between different sublattices. Here sublattices A and B are color-coded in blue and red to make the equations more amenable to visual parsing. In this chapter i and j will be exclusively referring to cites on sublattice A and B respectively and will be color-coded accordingly as $i \in A$ and $j \in B$. For example hopping term from lattice A to lattice B is written as $t_{A \leftarrow B} \equiv t_{ij}$. Nearest neighbors are denoted as $\langle i, j \rangle$ and σ is a label for spin.

$$\mathrm{H}_{\text{free}} = \sum_{\langle i,j \rangle \sigma} t_{ij} c^{\dagger}_{i\sigma} c_{j\sigma} + h.c. + \Delta_{ij} c^{\dagger}_{i\sigma} c^{\dagger}_{j\sigma} + h.c. \tag{4.1}$$

Furthermore Hubbard interaction at half filling is defined using the spin degrees of freedom.

$$\mathrm{H}_{\text{hubbard}} = U \sum_{l} \left(n_{l\uparrow} - \frac{1}{2} \right) \left(n_{l\downarrow} - \frac{1}{2} \right) \tag{4.2}$$

For a homogeneous case $t_{ij} = t$ and $\Delta_{ij} = \Delta$.

4.2 Majorana Basis

To solve this problem Majorana basis is introduced [19],

$$c_{i\sigma} = \eta_{i\sigma} + i\beta_{i\sigma} \tag{4.3}$$
$$c_{j\sigma} = \beta_{j\sigma} + i\eta_{j\sigma} \tag{4.4}$$

With this the Hamiltonian is rewritten term-by-term (see C.3)

$$t c^{\dagger}_{i\sigma} c_{j\sigma} + h.c. = 2it\eta_{i\sigma}\eta_{j\sigma} - 2it\beta_{i\sigma}\beta_{j\sigma} \tag{4.5}$$

$$\Delta c^{\dagger}_{i\sigma} c^{\dagger}_{j\sigma} + h.c. = -2i\Delta\eta_{i\sigma}\eta_{j\sigma} - 2i\Delta\beta_{i\sigma}\beta_{j\sigma} \tag{4.6}$$

$$\left(n_{l\uparrow} - \frac{1}{2}\right)\left(n_{l\downarrow} - \frac{1}{2}\right) = (2i\beta_{l\uparrow}\eta_{l\uparrow})(2i\beta_{l\downarrow}\eta_{\downarrow}) \tag{4.7}$$

Resulting in

$$\mathrm{H}_0 = \sum_{\langle i,j\rangle\sigma} 2i(t-\Delta)\eta_{i\sigma}\eta_{j\sigma} - 2i(t+\Delta)\beta_{i\sigma}\beta_{j\sigma} \tag{4.8}$$

$$\mathrm{H}_{\mathrm{int}} = -U\sum_{l}(2i\beta_{l\uparrow}\beta_{l\downarrow})(2i\eta_{l\uparrow}\eta_{l\downarrow}) \tag{4.9}$$

Rewrite the parameters

$$t + \Delta = 2\tilde{t} \qquad \frac{t-\Delta}{t+\Delta} \equiv \delta \tag{4.10}$$

and introduce new operator

$$D_l = 4i\eta_{l\uparrow}\eta_{l\downarrow} \tag{4.11}$$

to arrive at

$$\mathrm{H}_0 = 4i\tilde{t}\sum_{\langle i,j\rangle\sigma} \delta\eta_{i\sigma}\eta_{j\sigma} - \beta_{i\sigma}\beta_{j\sigma} \tag{4.12}$$

$$\mathrm{H}_{\mathrm{int}} = -U\sum_{l} D_l(i\beta_{l\uparrow}\beta_{l\downarrow}) \tag{4.13}$$

4.3 Symmetric lines

In the case of $\delta = 0$ (or $t = \Delta$) Hamiltonian no longer contains terms with η's and $[D_l, \mathrm{H}] = 0$ for all l, meaning it is a conserved quantity. Eigenvalues can be found by noting that

$$D_l^2 = (4i\eta_{l\uparrow}\eta_{l\downarrow})(4i\eta_{l\uparrow}\eta_{l\downarrow}) = 16\eta_{l\uparrow}^2\eta_{l\downarrow}^2 = 16\frac{1}{4}\frac{1}{4} = 1$$

Hence the eigenvalues of D_l are ± 1. Different sectors of Hilbert space can be labeled with different $\{D_l\}$ configurations for a total of 2^N sectors, where N is the number of lattice cites. Each sector is described by an effective Hamiltonian where the corresponding replacement $D_l \mapsto \pm 1$ in (4.13) is made. This Hamiltonian is quadratic and therefore diagonalizable. Interestingly $D \equiv \sum_l D_l$ is still conserved when $\delta \neq 0$. To check this only one commutator needs to be calculated

$$\begin{aligned}
\left[4i\tilde{t}\sum_{\langle i,j\rangle\sigma}\delta\eta_{i\sigma}\eta_{j\sigma}, \sum_l D_l\right] &= -16\tilde{t}\delta\sum_{\langle i,j\rangle\sigma l}[\eta_{i\sigma}\eta_{j\sigma}, \eta_{l\uparrow}\eta_{l\downarrow}] \\
&= -16\tilde{t}\delta\sum_{\langle i,j\rangle\sigma l}\eta_{i\sigma}[\eta_{j\sigma}, \eta_{l\uparrow}\eta_{l\downarrow}] + [\eta_{i\sigma}, \eta_{l\uparrow}\eta_{l\downarrow}]\eta_{j\sigma} \\
&= -16\tilde{t}\delta\sum_{\langle i,j\rangle\sigma l}\eta_{i\sigma}\{\eta_{j\sigma}, \eta_{l\uparrow}\}\eta_{l\downarrow} - \eta_{i\sigma}\eta_{l\uparrow}\{\eta_{j\sigma}, \eta_{l\downarrow}\} \\
&\qquad + \{\eta_{i\sigma}, \eta_{l\uparrow}\}\eta_{l\downarrow}\eta_{j\sigma} - \eta_{l\uparrow}\{\eta_{i\sigma}, \eta_{l\downarrow}\}\eta_{j\sigma}
\end{aligned}$$

$$= -8\tilde{t}\delta \sum_{\langle i,j \rangle} \eta_{i\uparrow}\eta_{j\downarrow} - \eta_{i\downarrow}\eta_{j\uparrow} + \eta_{i\downarrow}\eta_{j\uparrow} - \eta_{i\uparrow}\eta_{j\downarrow} = 0$$

Physical significance of this conserved quantity is discussed in later sections.

4.4 Composite fermions

Working in Majorana basis is useful, however, a better choice is composite fermion basis defined as

$$d_{i1} = \beta_{i\uparrow} - i\beta_{i\downarrow} \qquad d_{j1} = \beta_{j\uparrow} + i\beta_{j\downarrow} \tag{4.14}$$

$$d_{i2} = \eta_{i\uparrow} + i\eta_{i\downarrow} \qquad d_{j2} = \eta_{j\uparrow} - i\eta_{j\downarrow} \tag{4.15}$$

Rewrite Hamiltonian term-by-term (see C.4)

$$4\beta_{i\uparrow}\beta_{j\uparrow} + 4\beta_{i\downarrow}\beta_{j\downarrow} = 2d_{i1}d_{j1} + 2d_{i1}^{\dagger}d_{j1}^{\dagger} \tag{4.16}$$

$$4\eta_{i\uparrow}\eta_{j\uparrow} + 4\eta_{i\downarrow}\eta_{j\downarrow} = 2d_{l2}d_{l2} + 2d_{l2}^{\dagger}d_{l2}^{\dagger} \tag{4.17}$$

$$(2i\beta_{l\uparrow}\beta_{l\downarrow})(2i\eta_{l\uparrow}\eta_{l\downarrow}) = -\left(n_{l1} - \frac{1}{2}\right)\left(n_{l2} - \frac{1}{2}\right) \tag{4.18}$$

Here $n \equiv d^{\dagger}d$ is the number operator for composite d-fermions. Hamiltonian takes the following form

$$\mathrm{H}_0 = 2i\tilde{t} \sum_{\langle i,j \rangle} \delta(2d_{i2}d_{j2} + 2d_{i2}^{\dagger}d_{j2}^{\dagger}) - (2d_{i1}d_{j1} + 2d_{i1}^{\dagger}d_{j1}^{\dagger}) \tag{4.19}$$

$$\mathrm{H}_{\mathrm{int}} = U \sum_{l} \left(n_{l1} - \frac{1}{2}\right)\left(n_{l2} - \frac{1}{2}\right) \tag{4.20}$$

Note that the effective Hamiltonian only contains SC pairings and no hopping terms. Conserved quantity D_l becomes

$$D_l = \xi_l(2n_{l2} - 1) \quad \text{where} \quad \xi_l = \begin{cases} +1 & l \in A \\ -1 & l \in B \end{cases} \tag{4.21}$$

Introduction of ξ_l is necessary to properly write down the transformation from Majorana to composite fermion basis. Hilbert space sectors can be labeled by $\xi_l D_l$. In the limit $\delta = 0$ Hamiltonian becomes

$$\mathrm{H} = -4i\tilde{t} \sum_{\langle i,j \rangle} d_{i1}d_{j1} + d_{i1}^{\dagger}d_{j1}^{\dagger} + U \sum_{l} \xi_l D_l \left(n_{l1} - \frac{1}{2}\right) \tag{4.22}$$

Interestingly non-interacting part of this Hamiltonian is the same as (4.1) with complex nearest neighbor SC pairing, with obvious caveat that this Hamiltonian is written in composite fermion basis.

4.5 Explicit transformation $c \to d$

For completeness transformation from c to d fermions is written out explicitly. (see appendix C.4 for complete derivation)

$$d_{i1} = \frac{1}{i\sqrt{2}}(c_{i\leftarrow} - c^\dagger_{i\rightarrow}) \qquad d_{i2} = \frac{1}{\sqrt{2}}(c_{i\rightarrow} + c^\dagger_{i\leftarrow})$$
$$d_{j1} = \frac{1}{\sqrt{2}}(c_{j\rightarrow} + c^\dagger_{j\leftarrow}) \qquad d_{j2} = \frac{1}{i\sqrt{2}}(c_{j\leftarrow} - c^\dagger_{j\rightarrow})$$

Notation $c_\leftarrow$ and $c_\rightarrow$ comes from the eigenvalues of Pauli matrices σ_y and σ_z which describe polarizations of spin along $\hat{y}$ and $\hat{z}$ axes respectively (see C.4). Let

$$d_{l\rightarrow} = \frac{1}{\sqrt{2}}(c_{l\rightarrow} + c^\dagger_{l\leftarrow}) \tag{4.23}$$
$$d_{l\leftarrow} = \frac{1}{i\sqrt{2}}(c_{l\leftarrow} - c^\dagger_{l\rightarrow}) \tag{4.24}$$

d-fermions are a particle-hole superposition of $\hat{y}$-polarized c-fermions on the same lattice site. D_l can now be interpreted as a little better now

$$D_l = \begin{cases} (2n_{l\rightarrow} - 1) & l \in A \\ -(2n_{l\leftarrow} - 1) & l \in B \end{cases}$$

It measures spin and its sign. On sublattice A it measures total spin right and on B - left. So the sum D measures how staggered the magnetization along $\hat{y}$-axis is.

4.6 Eigenstates of $n_{l\leftarrow}$ and $n_{l\rightarrow}$

In order to apply perturbation theory to a Hamiltonian one needs to know its unperturbed eigenstates. We start construction by first vacuum state must be defined. d-fermion vacuum is generally different from c-fermion vacuum. It is labeled as $|0\rangle_d$. By definition

$$d_\leftarrow|0\rangle_d = d_\rightarrow|0\rangle_d = 0 \tag{4.25}$$

Using (4.23) following condition is derived

$$c_\rightarrow|0\rangle_d = -c^\dagger_\leftarrow|0\rangle_d \tag{4.26}$$
$$c_\leftarrow|0\rangle_d = c^\dagger_\rightarrow|0\rangle_d \tag{4.27}$$

Use this to find the projection on c-fermion states

$$\langle 0|c_\leftarrow|0\rangle_d = -\langle 0|c^\dagger_\rightarrow|0\rangle_d = 0 \tag{4.28}$$
$$\langle 0|c_\rightarrow|0\rangle_d = \langle 0|c^\dagger_\leftarrow|0\rangle_d = 0 \tag{4.29}$$
$$\langle 0|c_\rightarrow c_\leftarrow|0\rangle_d = \langle 0|c_\rightarrow c^\dagger_\rightarrow|0\rangle_d = \langle 0|\{c_\rightarrow, c^\dagger_\rightarrow\}|0\rangle_d = \langle 0|0\rangle_d \tag{4.30}$$

Using the normalization condition we find for a single site

$$|0\rangle_d = \frac{1}{\sqrt{2}}(1 + c^\dagger_{\leftarrow} c^\dagger_{\rightarrow})|0\rangle \tag{4.31}$$

This is a form of a local Bogoliubov transformation. Ground state can be fount by taking a direct product of vacuum states of individual lattice cites.

$$|0\rangle_d = \prod_l \frac{1}{\sqrt{2}}(1 + c^\dagger_{l\leftarrow} c^\dagger_{l\rightarrow})|0\rangle \tag{4.32}$$

One and multiparticle states can be created by acting with $d^\dagger$ operators on d-fermion vacuum. This set of states is an eigensystem for D_l and $\xi_l D_l$. (see C.5)

CHAPTER 5

BCS-Hubbard Nanoribbon

Carbon nanoribbons are made by cutting graphene into strips. In this work two types of ribbons are considered: armchair and zigzag. These differ by their edges and exhibit different properties. Zigzag ribbon has edge states and flatbands which make it potentially interesting to study from topological point of view. However this work focuses on armchair as it is less explored in the literature.

5.1 Zigzag Nanoribbon(ZNR)

5.1.1 Model Hamiltonian

Similar to armchair nanoribbon, unit cell of a zigzag ribbon is denoted on fig. 5.1 with dashed lines and has length $a\sqrt{3}$. Width of the ribbon is N and the length is taken to be L_y. PBC are assumed along $\hat{y}$-axis. Similarly to armchair case a Hamiltonian is constructed with operators $a^\dagger_{lm}/b^\dagger_{lm}$ that create electrons at unit cell l and position $m\mathrm{A}/m\mathrm{B}$, hopping terms have strength $-t$.

$$\mathrm{H} = -t\sum_l \left[\sum_{m\in\text{even}} a^\dagger_l(m)b_{l-1}(m) + \sum_{m\in\text{odd}} a^\dagger_{l-1}(m)b_l(m)\right] \tag{5.1}$$

$$-t\sum_l\sum_{m=1}^{N} a^\dagger_l(m)b_l(m) \tag{5.2}$$

$$-t\sum_l\sum_{m=1}^{N-1} a^\dagger_l(m+1)b_l(m) + h.c. \tag{5.3}$$

To this are added SC pairing terms with strength $-\Delta$

$$\mathrm{H}_{SC} = -\Delta\sum_l \left[\sum_{m\in\text{even}} a^\dagger_l(m)b_{l-1}(m) + \sum_{m\in\text{odd}} a^\dagger_{l-1}(m)b_l(m)\right] \tag{5.4}$$

$$-\Delta\sum_l\sum_{m=1}^{N} a^\dagger_l(m)b_l(m) \tag{5.5}$$

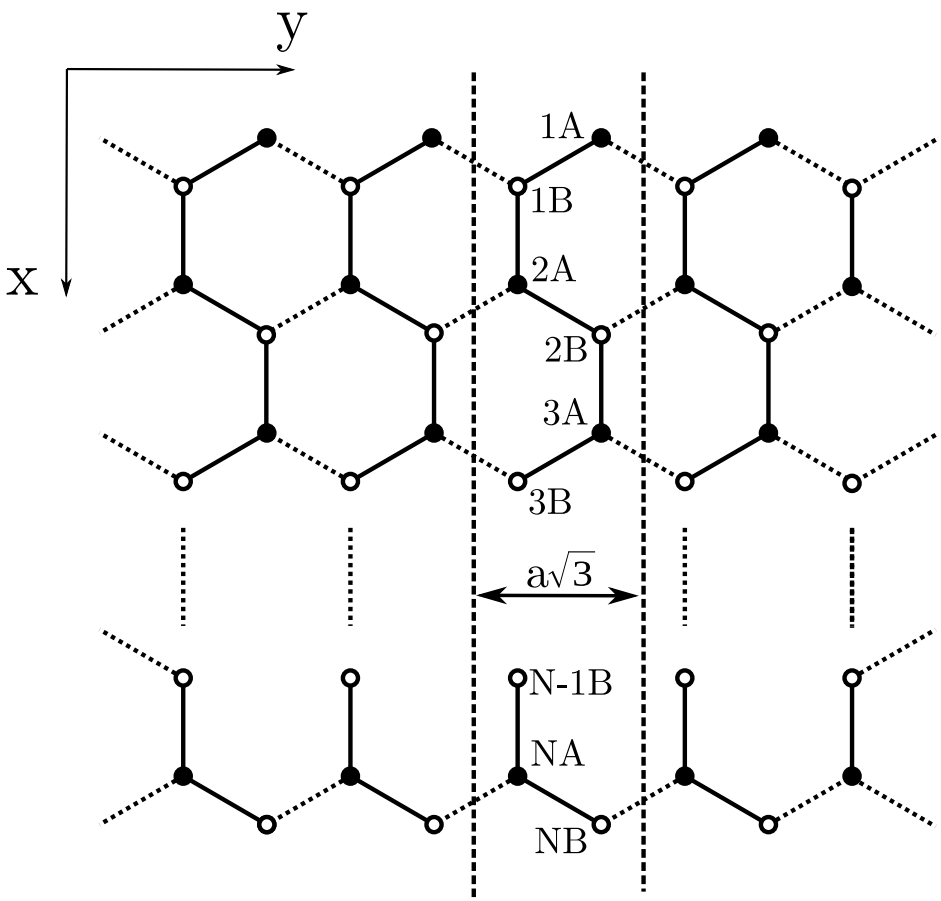

Figure 5.1: Lattice of an zigzag carbon nanoribbon, with unit cell(dashed) of size $a\sqrt{3}$, width N and length L_y

$$-\Delta \sum_{l} \sum_{m=1}^{N-1} a_l^{\dagger}(m+1) b_l(m) + h.c. \tag{5.6}$$

as well as spin degrees of freedom σ. Operators are rewritten in the same way as in section 4.1

$$a_l(m) \mapsto c^{a}_{lm\sigma} \qquad b_l(m) \mapsto c^{b}_{lm\sigma} \tag{5.7}$$

Solution is found by going to composite d-fermion basis. Consider case $\delta = 0$

$$\mathrm{H} = 4\tilde{t} \sum_{l} \left[\sum_{m \in \text{even}} i d^{a}_{lm} d^{b}_{l-1m} + \sum_{m \in \text{odd}} i d^{a}_{l-1m} d^{b}_{lm} \right] \tag{5.8}$$

$$+4\tilde{t} \sum_{l} \sum_{m=1}^{N} i d^{a}_{lm} d^{b}_{lm} + 4\tilde{t} \sum_{l} \sum_{m=1}^{N-1} i d^{a}_{lm+1} d^{b}_{lm} + h.c. \tag{5.9}$$

$$\mathrm{H}_{\text{int}} = U \sum_{l} \xi_l D_l \left(n_l - \frac{1}{2} \right) \tag{5.10}$$

5.1.2 Fourier Transform

Due to PBC Fourier transform is introduced along $\hat{y}$-axis.

$$d^a_{lm} = \frac{1}{\sqrt{L_y}} \sum_k e^{iky_{lma}} d^a_{km} \qquad d^b_{lm} = \frac{1}{\sqrt{L_y}} \sum_k e^{iky_{lmb}} d^b_{km} \tag{5.11}$$

with

$$y_{lma} \equiv y_l \qquad \text{for } m \text{ odd} \tag{5.12}$$
$$y_{lmb} = y_l - a\sin(\pi/3) \qquad \text{for } m \text{ odd} \tag{5.13}$$
$$y_{lma} = y_l - a\sin(\pi/3) \qquad \text{for } m \text{ even} \tag{5.14}$$
$$y_{lmb} = y_l \qquad \text{for } m \text{ even} \tag{5.15}$$

as well as

$$y_{l+1} = y_l + a\sqrt{3} \tag{5.16}$$

These relations are easy to derive from fig. 5.1. We transform the Hamiltonian term-by-term (see D.2) and redefine d-fermion operators as follows

$$e^{ika\sqrt{3}/2} d^a_{-km} \mapsto d^a_{-km} \quad m \in \text{even} \tag{5.17}$$
$$e^{-ika\sqrt{3}/2} d^a_{-km} \mapsto d^a_{-km} \quad m \in \text{odd} \tag{5.18}$$

After simple algebra one arrives at

$$\mathrm{H} = 4\tilde{t} \sum_k \sum_{m=1}^{N} 2i\cos(\sqrt{3}ka/2) d^a_{-km} d^b_{km} + h.c. \tag{5.19}$$
$$+ 4\tilde{t} \sum_k \sum_{m=1}^{N-1} i d^a_{-km+1} d^b_{km} + h.c. \tag{5.20}$$
$$+ U \sum_k \sum_{m=1}^{N} D_{am} \left({d^a}^\dagger_{-km} d^a_{-km} - \frac{1}{2} \right) - D_{bm} \left({d^b}^\dagger_{km} d^b_{km} - \frac{1}{2} \right) \tag{5.21}$$

D_l is rewritten as D_{am} and D_{bm}

5.1.3 Matrix form

Introduce vectors

$$d^\lambda_k = \begin{pmatrix} d^\lambda_{k1} & d^\lambda_{k2} & \cdots d^\lambda_{kN} \end{pmatrix}^T \tag{5.22}$$

and

$$d_k = \begin{pmatrix} d^a_{-k} \\ {d^a}^\dagger_{-k} \\ d^b_k \\ {d^b}^\dagger_k \end{pmatrix} \qquad d^\dagger_k = \begin{pmatrix} {d^a}^\dagger_{-k} & d^a_{-k} & {d^b}^\dagger_k & d^b_k \end{pmatrix} \tag{5.23}$$

Similar to how we did in 3.3 we write the Hamiltonian in a symmetric form

$$\mathrm{H}_0 = 2\tilde{t}\sum_k\sum_{m=1}^{N} 2i\cos(\sqrt{3}ka/2)(d^a_{-km}d^b_{km} - d^b_{km}d^a_{-km}) + h.c. \tag{5.24}$$

$$+ 2\tilde{t}\sum_k\sum_{m=1}^{N-1} id^a_{-km+1}d^b_{km} - id^b_{km}d^a_{-km+1} + h.c. \tag{5.25}$$

$$+ \frac{U}{2}\sum_k\sum_{m=1}^{N} D_{am}({d^a}^\dagger_{-km}d^a_{-km} - d^a_{-km}{d^a}^\dagger_{-km}) - D_{bm}({d^b}^\dagger_{km}d^b_{km} - d^b_{km}{d^b}^\dagger_{km}) \tag{5.26}$$

Furthermore define

$$\mathrm{H} = \sum_k d^\dagger_k \mathrm{H}_k d_k \tag{5.27}$$

with

$$\mathrm{H}_k = \begin{pmatrix} \frac{U}{2}D_{am} & 0 & 0 & 2i\tilde{t}(g_k\mathbb{1}+\mathbb{K}) \\ 0 & -\frac{U}{2}D_{am} & 2i\tilde{t}(g_k\mathbb{1}+\mathbb{K}) & 0 \\ 0 & -2i\tilde{t}(g_k\mathbb{1}+\mathbb{K}^\dagger) & -\frac{U}{2}D_{bm} & 0 \\ -2i\tilde{t}(g_k\mathbb{1}+\mathbb{K}^\dagger) & 0 & 0 & \frac{U}{2}D_{bm} \end{pmatrix} \tag{5.28}$$

and

$$g_k = 2\cos\left(\frac{\sqrt{3}ka}{2}\right) \qquad \mathbb{K} = \begin{pmatrix} 0 & 1 & \cdots & & 0 \\ 0 & 0 & & & \\ \vdots & & \ddots & & \vdots \\ & & & 0 & 1 \\ 0 & & \cdots & 0 & 0 \end{pmatrix} \tag{5.29}$$

We can also write it more compactly as

$$H = -\frac{U}{2}D\otimes\sigma_z - 2\tilde{t}\mathbb{1}\otimes\sigma_y\otimes\sigma_x + i\tilde{t}g_k\mathbb{K}\otimes\sigma^+\otimes\sigma_x - i\tilde{t}g_k\mathbb{K}^\dagger\otimes\sigma^-\otimes\sigma_x \tag{5.30}$$

Here σ's are Pauli matrices that act on the sub-lattice and particle-hole spaces. Matrix D depends on the section of the Hilbert space. $\sigma^\pm \equiv (\sigma_x \pm i\sigma_y)/2$ are the raising and lowering operators for half-integer spin. In the limit $U = 0$ we get fig. 5.2 An obvious property of the zigzag nanoribbons is the flatband in the middle third of the Brillouin zone, which correspond to the edge states in physical space. By adding different interactions these edge states can be made topological wherein they become chiral and we observe opposite spin currents on opposite edges [17], [18]. All energy levels are doubly degenerate.

Antiferromagnetic(AF) order

In the ground state $D_{am} = -D_{bm} = -1$ or $D = \mathbb{1}\otimes\mathbb{1}$ (see C.5). This shall be referred to as *AF order*, since in this sector of Hilbert space both sub-lattices are populated by d_2-fermions and on different

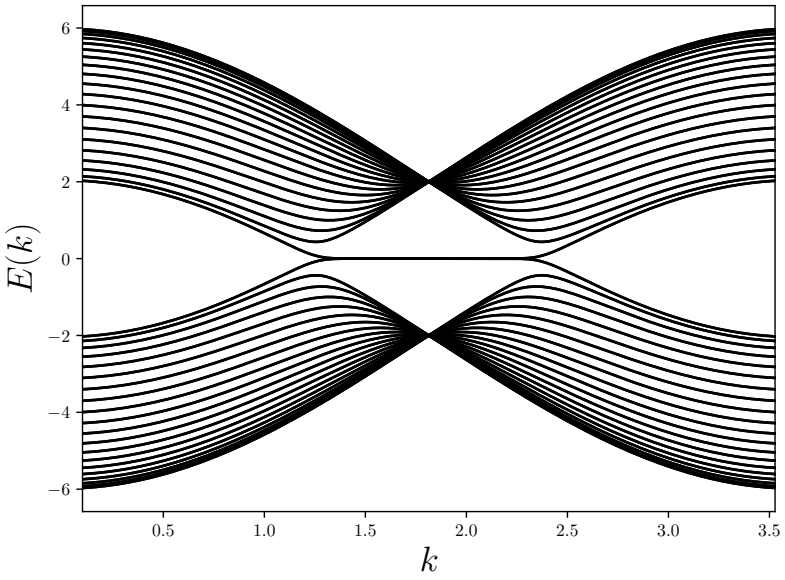

Figure 5.2: Energy levels of the zigzag nanoribbon. $E(k)$ and k are given in the units of $\tilde{t}$

sub-lattices d_2 has opposite y-polarizations. Now the matrix can be written as

$$\mathrm{H}_k = \begin{pmatrix} -\frac{U}{2} & 0 & 0 & 2i\tilde{t}(g_k\mathbb{1}+\mathbb{K}) \\ 0 & \frac{U}{2} & 2i\tilde{t}(g_k\mathbb{1}+\mathbb{K}) & 0 \\ 0 & -2i\tilde{t}(g_k\mathbb{1}+\mathbb{K}^\dagger) & -\frac{U}{2} & 0 \\ -2i\tilde{t}(g_k\mathbb{1}+\mathbb{K}^\dagger) & 0 & 0 & \frac{U}{2} \end{pmatrix} \tag{5.31}$$

Energy levels are given in fig. 5.3(a). We observe gap opening however the degeneracy is not lifted and every level is still doubly degenerate.

Ferromagnetic(F) order

Ferromagnetic in this context means we are considering the sector of Hilbert space where only one sub-lattice is populated by d_2-fermions. It corresponds to the state in which all d_2 fermions are aligned $\otimes_l |l \leftarrow\rangle_d$ or $\otimes_l |l \rightarrow\rangle_d$. Now the matrix looks like

$$\mathrm{H}_k = \begin{pmatrix} \mp\frac{U}{2} & 0 & 0 & 2i\tilde{t}(g_k\mathbb{1}+\mathbb{K}) \\ 0 & \pm\frac{U}{2} & 2i\tilde{t}(g_k\mathbb{1}+\mathbb{K}) & 0 \\ 0 & -2i\tilde{t}(g_k\mathbb{1}+\mathbb{K}^\dagger) & \pm\frac{U}{2} & 0 \\ -2i\tilde{t}(g_k\mathbb{1}+\mathbb{K}^\dagger) & 0 & 0 & \mp\frac{U}{2} \end{pmatrix} \tag{5.32}$$

Since the spectrum is symmetric ± doesn't change anything, and after solving for the eigenvalues and plotting them w.r.t. momenta (fig. 5.3(a)) one can see energy level splitting.

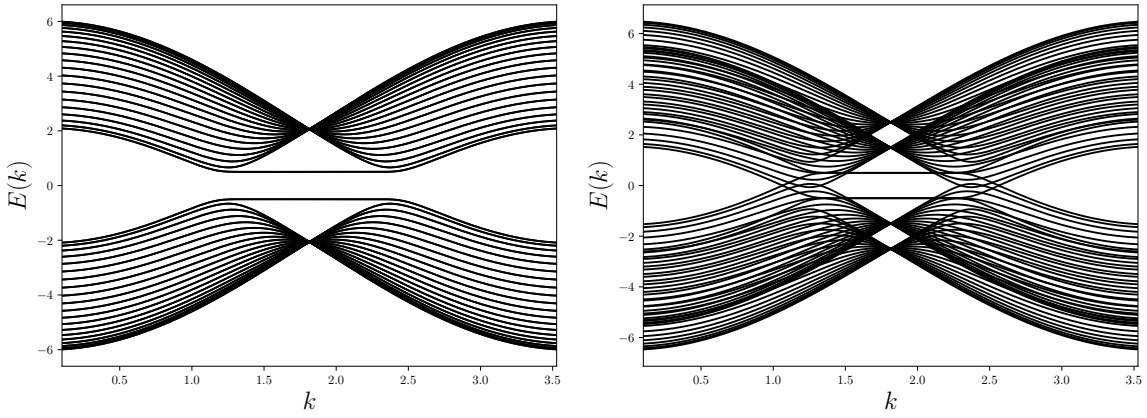

(a) Antiferromagnetic order

(b) Ferromagnetic order

Figure 5.3: Zigzag energy levels for F and AF orders. $E(k)$ and k are measured in units of $\tilde{t}$. Calculation is done for $N = 20$, $U = 1$

5.2 Armchair Nanoribbon(ANR)

5.2.1 Model Hamiltonian

Unit cell is shown on the fig. 5.4 with dashed lines. It has the size $3a$. Width of the ribbon is given by N. Length of the ribbon is taken to be L_y. Periodic boundary conditions are assumed along $\hat{y}$-axis. Let $a^\dagger_{lm}/b^\dagger_{lm}$ create electrons at unit cell l and position mA/mB, with hopping terms having strength $-t$. This leads to the Hamiltonian which is given in [20]

$$\mathrm{H} = -t \sum_l \left[\sum_{m\in\text{odd}} a^\dagger_l(m) b_{l-1}(m) + \sum_{m\in\text{even}} a^\dagger_l(m) b_l(m) \right] + h.c. \tag{5.33}$$

$$-t \sum_l \sum_{m=1}^{N-1} a^\dagger_l(m) b_l(m+1) + a^\dagger_l(m+1) b_l(m) + h.c. \tag{5.34}$$

To this are added SC pairing terms with strength $-\Delta$

$$\mathrm{H}_{SC} = -\Delta \sum_l \left[\sum_{m\in\text{odd}} a^\dagger_l(m) b^\dagger_{l-1}(m) + \sum_{m\in\text{even}} a^\dagger_l(m) b^\dagger_l(m) \right] + h.c. \tag{5.35}$$

$$-\Delta \sum_l \sum_{m=1}^{N-1} a^\dagger_l(m) b^\dagger_l(m+1) + a^\dagger_l(m+1) b^\dagger_l(m) + h.c. \tag{5.36}$$

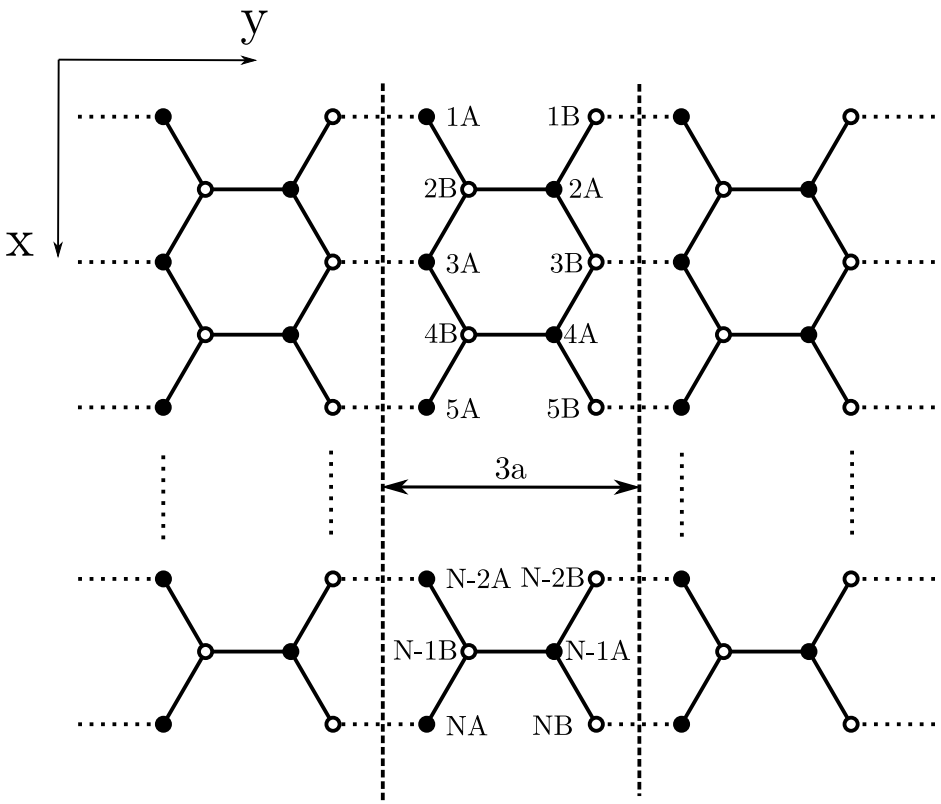

Figure 5.4: Lattice of an armchair carbon nanoribbon, with unit cell(dashed) of size $3a$, width N and length L_y

as well as spin degrees of freedom σ. Operators are written it the same way as in section 4.1

$$a_l(m) \mapsto c^a_{lm\sigma} \qquad b_l(m) \mapsto c^b_{lm\sigma} \tag{5.37}$$

This system is solved using the insights from previous sections, viz. for a bipartite lattice with SC pairing and Hubbard interaction Hamiltonian can be simplified by going to composite fermion basis. Consider case $\delta = 0$

$$\mathrm{H}_0 = 4\tilde{t} \sum_l \left[\sum_{m\in\mathrm{odd}} i d^a_{lm} d^b_{l-1m} + \sum_{m\in\mathrm{even}} i d^a_{lm} d^b_{lm} \right] + h.c. \tag{5.38}$$

$$+ 4\tilde{t} \sum_l \sum_{m=1}^{N-1} i d^a_{lm} d^b_{lm+1} + i d^a_{lm+1} d^b_{lm} + h.c. \tag{5.39}$$

$$\mathrm{H}_{\mathrm{int}} = U \sum_l \xi_l D_l \left(n_l - \frac{1}{2} \right) \tag{5.40}$$

For brevity d_1 is renamed to d, since case $\delta = 0$ means that d_2 fermions have no kinetic terms and don't appear outside of D_l.

5.2.2 Fourier Transform

Fourier transform along $\hat{y}$-axis is written as

$$d^a_{lm} = \frac{1}{\sqrt{L_y}} \sum_k e^{iky_{lma}} d^a_{km} \qquad d^b_{lm} = \frac{1}{\sqrt{L_y}} \sum_k e^{iky_{lmb}} d^b_{km} \tag{5.41}$$

with

$$y_{lma} \equiv y_l \qquad \text{for } m \text{ odd} \tag{5.42}$$
$$y_{lmb} = y_l + 2a \qquad \text{for } m \text{ odd} \tag{5.43}$$
$$y_{lma} = y_l + a\cos(\pi/3) + a \qquad \text{for } m \text{ even} \tag{5.44}$$
$$y_{lmb} = y_l + a\cos(\pi/3) \qquad \text{for } m \text{ even} \tag{5.45}$$

as well as

$$y_{l+1} = y_l + 3a \tag{5.46}$$

These relations are easy to see from fig. 5.4. Transform the Hamiltonian term-by-term (see D.1)

$$\sum_l \left(\sum_{m\in\text{odd}} d^a_{lm} d^b_{l-1m} + \sum_{m\in\text{even}} d^a_{lm} d^b_{lm} \right) = \sum_k \sum_{m=1}^{N} e^{-ika} d^a_{-km} d^b_{km} \tag{5.47}$$

$$\sum_l \sum_{m=1}^{N-1} d^a_{lm+1} d^b_{lm} = \sum_k \sum_{m=1}^{N-1} e^{-ika} e^{ika_T/2} d^a_{-km+1} d^b_{km} \tag{5.48}$$

$$\sum_{lm} {d^{\lambda}}^{\dagger}_{lm} d^{\lambda}_{lm} = \sum_{mk} {d^{\lambda}}^{\dagger}_{km} d^{\lambda}_{km} \tag{5.49}$$

Absorb the extra phase factor by redefining $e^{-ika} {d^a}_{-km} \mapsto {d^a}_{-km}$. This doesn't affect Hubbard interaction since it has terms of the form $d^\dagger d$ and the phases cancel out. Now one arrives at

$$\mathrm{H} = 4\tilde{t} \sum_k \sum_{m=1}^{N} i d^a_{-km} d^b_{km} + h.c. \tag{5.50}$$

$$+ 4\tilde{t} \sum_k \sum_{m=1}^{N-1} i e^{ika_T/2} (d^a_{-km} d^b_{km+1} + d^a_{-km+1} d^b_{km}) + h.c. \tag{5.51}$$

$$+ U \sum_k \sum_{m=1}^{N} D_{am} \left({d^a}^{\dagger}_{km} d^a_{-km} - \frac{1}{2} \right) - D_{bm} \left({d^b}^{\dagger}_{km} d^b_{km} - \frac{1}{2} \right) \tag{5.52}$$

D_l is rewritten as D_{am} and D_{bm}

5.2.3 Matrix form

Introduce vectors

$$d_k^\lambda = \begin{pmatrix} d_{k1}^\lambda & d_{k2}^\lambda & \cdots d_{kN}^\lambda \end{pmatrix}^T \tag{5.53}$$

and

$$d_k = \begin{pmatrix} d_{-k}^a \\ d_{-k}^{a\dagger} \\ d_k^b \\ d_k^{b\dagger} \end{pmatrix} \qquad d_k^\dagger = \begin{pmatrix} d_{-k}^{a\dagger} & d_{-k}^a & d_k^{b\dagger} & d_k^b \end{pmatrix} \tag{5.54}$$

Similar to how it is done in 3.3 Hamiltonian is written in a symmetric form

$$\mathrm{H} = 2\tilde{t} \sum_k \sum_{m=1}^{N} i d_{-km}^a d_{km}^b - i d_{km}^b d_{-km}^a + h.c. \tag{5.55}$$

$$+ 2\tilde{t} \sum_k \sum_{m=1}^{N-1} i e^{ika_T/2} (d_{-km}^a d_{km+1}^b + d_{-km+1}^a d_{km}^b - d_{km+1}^b d_{-km}^a - d_{km}^b d_{-km+1}^a) + h.c. \tag{5.56}$$

$$+ \frac{U}{2} \sum_k \sum_{m=1}^{N} D_{am} (d^{a\dagger}_{-km} d_{-km}^a - d_{-km}^a d^{a\dagger}_{-km}) - D_{bm} (d^{b\dagger}_{km} d_{km}^b - d_{km}^b d^{b\dagger}_{km}) \tag{5.57}$$

Furthermore define

$$\mathrm{H} = \sum_k d_k^\dagger \mathrm{H}_k d_k \tag{5.58}$$

with

$$\mathrm{H}_k = \begin{pmatrix} \frac{U}{2} D_{am} & 0 & 0 & 2i\tilde{t}(\mathbb{1} + e^{-ika_t/2}\mathbb{J}) \\ 0 & -\frac{U}{2} D_{am} & 2i\tilde{t}(\mathbb{1} + e^{ika_t/2}\mathbb{J}) & 0 \\ 0 & -2i\tilde{t}(\mathbb{1} + e^{-ika_t/2}\mathbb{J}) & -\frac{U}{2} D_{bm} & 0 \\ -2i\tilde{t}(\mathbb{1} + e^{ika_t/2}\mathbb{J}) & 0 & 0 & \frac{U}{2} D_{bm} \end{pmatrix} \tag{5.59}$$

and

$$\mathbb{J} = \begin{pmatrix} 0 & 1 & \cdots & & 0 \\ 1 & 0 & & & \\ \vdots & & \ddots & & \vdots \\ & & & 0 & 1 \\ 0 & & \cdots & 1 & 0 \end{pmatrix} \tag{5.60}$$

We can also write this more compactly as

$$H = -\frac{U}{2} D \otimes \sigma_z - 2\tilde{t} \left(\mathbb{1} + \mathbb{J}\cos(ka_T/2)\right) \otimes \sigma_y \otimes \sigma_x - 2\tilde{t} \sin(ka_T/2) \mathbb{J} \otimes \sigma_y \otimes \sigma_y \tag{5.61}$$

Same as before D depends on the sector of the Hilbert space and Pauli matrices act on sub-lattice and particle-hole spaces. Unlike zigzag nanoribbons armchair geometry is width dependent, meaning

depending on N ribbon may behave as a semimetal or a semiconductor(fig. 5.5). Namely if the width is of the form $N = 3n - 1$ with $n \in \mathbb{Z}$ then we have a zero crossing at $k = 0$. In other cases there is an bandgap of the order $\sim 1/N$.

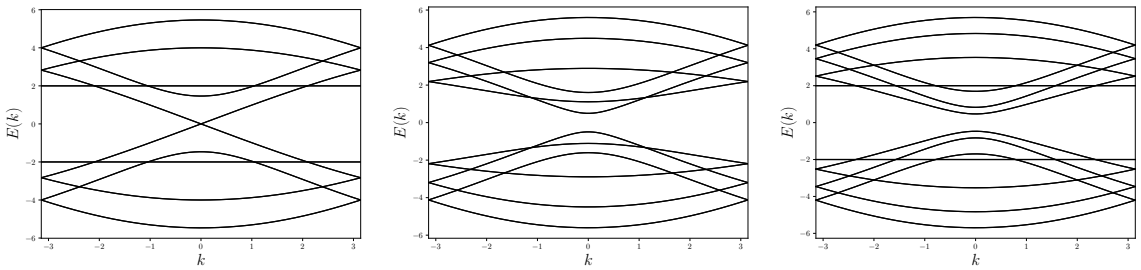

(a) N=5 (b) N=6 (c) N=7

Figure 5.5: Energy bands for widths 5,6,7 for the case $U = 0$. Everything is measured in units of $\tilde{t}$.

Antiferromagnetic(AF) order

As it was for zigzag configuration AF order here means $D_{am} = -D_{bm} = -1$ or $D = \mathbb{1} \otimes \mathbb{1}$(see C.5) and the matrix is rewritten as

$$\mathrm{H}_k = \begin{pmatrix} -\frac{U}{2} & 0 & 0 & 2i\tilde{t}(\mathbb{1} + e^{-ika_t/2}\mathbb{J}) \\ 0 & \frac{U}{2} & 2i\tilde{t}(\mathbb{1} + e^{ika_t/2}\mathbb{J}) & 0 \\ 0 & -2i\tilde{t}(\mathbb{1} + e^{-ika_t/2}\mathbb{J}) & -\frac{U}{2} & 0 \\ -2i\tilde{t}(\mathbb{1} + e^{ika_t/2}\mathbb{J}) & 0 & 0 & \frac{U}{2} \end{pmatrix} \tag{5.62}$$

Solving for the eigenvalues for every value of k and plotting the results gives the energy band structure 5.6(a), 5.6(b), 5.6(c). As with zigzag geometry here too we observe gap opening without lifting the degeneracy.

Ferromagnetic(F) order

Ferromagnetic as it was for zigzag nanoribbon mean we are considering the sector of Hilbert space where only one sub-lattice is populated by d_2-fermions, which in turn corresponds to the state in which all d_2 fermions are aligned $\otimes_l |l \leftarrow\rangle_d$ or $\otimes_l |l \rightarrow\rangle_d$, resulting in $D_{am} = D_{bm} = \pm 1$ or $D = \pm\mathbb{1} \otimes \sigma_z$(see C.5) Now the matrix looks like

$$\mathrm{H}_k = \pm \begin{pmatrix} \mp\frac{U}{2} & 0 & 0 & 2i\tilde{t}(\mathbb{1} + e^{-ika_t/2}\mathbb{J}) \\ 0 & \pm\frac{U}{2} & 2i\tilde{t}(\mathbb{1} + e^{ika_t/2}\mathbb{J}) & 0 \\ 0 & -2i\tilde{t}(\mathbb{1} + e^{-ika_t/2}\mathbb{J}) & \pm\frac{U}{2} & 0 \\ -2i\tilde{t}(\mathbb{1} + e^{ika_t/2}\mathbb{J}) & 0 & 0 & \mp\frac{U}{2} \end{pmatrix} \tag{5.63}$$

Since the spectrum is symmetric ± doesn't change anything. Solving for the eigenvalues and plotting it w.r.t. we can see the same behavior as in zigzag case. Degeneracy is lifted. For some widths there exists a critical value of $U = U_c$ where the bandgap closes, but if we keep increasing U eventually gap opens again and the bandstructure becomes that of a trivial insulator. Since band closing is unavoidable initial state must be topologically nontrivial.

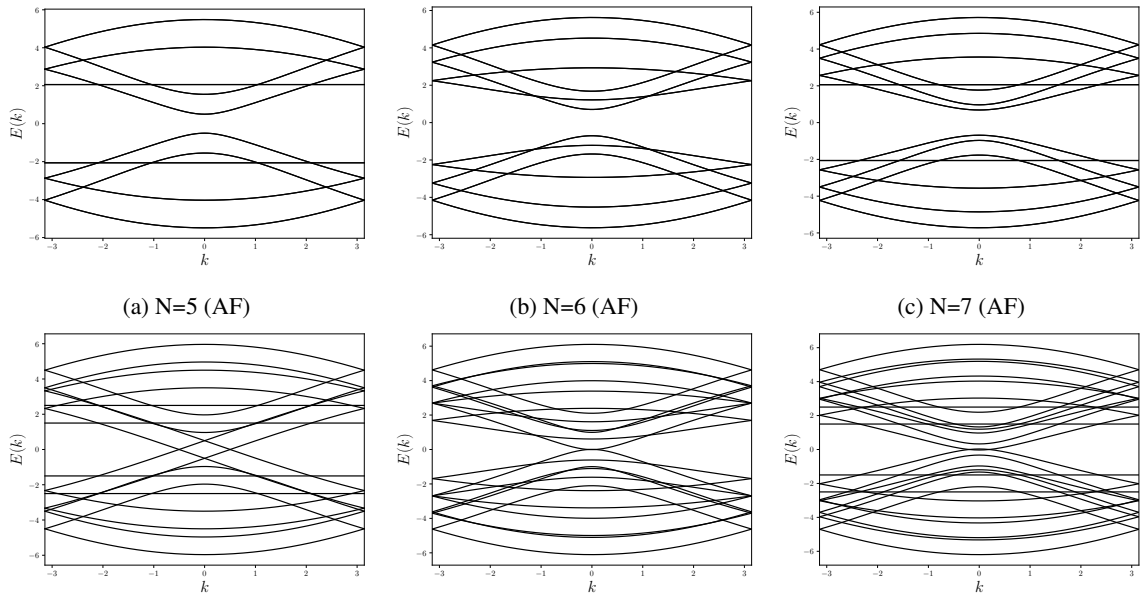

(a) N=5 (AF) (b) N=6 (AF) (c) N=7 (AF)

(d) N=5 (F) (e) N=6 (F) (f) N=7 (F)

Figure 5.6: Energy bands for widths 5,6,7 in both ferromagnetic and antiferromagnetic order. Everything is measured in units of $\tilde{t}$. For all calculations $U = 1$

5.3 Effective Hamiltonian

As we have seen the Hamiltonian can be written as

$$H_{\mathrm{ZNR}} = -\frac{U}{2} D \otimes \sigma_z - 2\tilde{t}\mathbb{1} \otimes \sigma_y \otimes \sigma_x + i\tilde{t} g_k \mathbb{K} \otimes \sigma^+ \otimes \sigma_x - i\tilde{t} g_k \mathbb{K}^\dagger \otimes \sigma^- \otimes \sigma_x \tag{5.64}$$

or

$$H_{\mathrm{ANR}} = -\frac{U}{2} D \otimes \sigma_z - 2\tilde{t}\left(\mathbb{1} + \mathbb{J}\cos(ka_T/2)\right) \otimes \sigma_y \otimes \sigma_x - 2\tilde{t}\sin(ka_T/2)\mathbb{J} \otimes \sigma_y \otimes \sigma_y \tag{5.65}$$

Matrix D depending on Hilbert space sector can take the form $D = \mathbb{1} \otimes \mathbb{1}$ or $D = \mathbb{1} \otimes \sigma_z$. Now we diagonalize the first term in the matrix product. Let $A \in \{\mathbb{J}, \mathbb{K}\}$ Then there exists a unitary transform such that

$$UAU^\dagger = \mathrm{diag}(\lambda_1, \lambda_2, \cdots) \tag{5.66}$$

where λ's are the eigenvalues and consequently

$$U(\mathbb{1} + A)U^\dagger = \mathrm{diag}(\lambda_1 + 1, \lambda_2 + 1, \cdots) \tag{5.67}$$

For every λ (5.64) and (5.65) become 4d Dirac equations, since direct product of Pauli matrices along with $2x2$ unit matrix spans Clifford algebra. In fact we are free to choose the basis $\{\Gamma_a\}_{a=1\cdots5}$ as long as it satisfies anticommutation relations

$$\{\Gamma_a, \Gamma_b\} = 2\delta_{ab} \qquad [\Gamma_a, \Gamma_b] = 2i\Gamma_{ab} \tag{5.68}$$

One possible choice is [21]

$$\{\sigma_x \otimes \mathbb{1},\ \sigma_z \otimes \mathbb{1},\ \sigma_y \otimes \sigma_x,\ \sigma_y \otimes \sigma_y,\ \sigma_y \otimes \sigma_z\} \tag{5.69}$$

CHAPTER 6

Conclusion and Discussion

In this work we present BCS-Hubbard Hamiltonian as a toy model to study topological properties on carbon nanoribbons. While studying the model new conserved quantities were discovered which was missed in the original paper as it only considered symmetric lines condition, whereas the new quantities are conserved in general case.

After applying the model to armchair geometry we for antiferromagnetic order gap opening in the bandstructure of nanoribbons. For ferromagnetic case, however, we observed gap closing and opening again as Hubbard interaction strength U is varied. Since the limit $U \to \infty$ leads to a trivial insulator and this limit cannot be reached without closing the energy gap we conclude that initial state is topological. Since the state is topological we want to find if there exist a topological conserved quantity. We intend to do it using 4D Dirac equation introduced at the end of the last chapter. Developing field theoretical approach may provide better insight into the nature of this system.

Moreover, nanoribbons of different geometries can be put together to produce more complex geometries with possibility of topological states existing at the junctions. We intend to investigate different configurations for interesting physics and their potential applications.

APPENDIX A

Group Theoretic proof of Bloch's Theorem

In the 2.3 we saw that the representation of $\mathbb{Z}$ is $U(1)$. In the *bulk* of the crystal this is self-evident, however, in the finite crystal the edges need special treatment. The assumption we chose was Born-von Karman periodic boundary conditions, namely if the crystal has length (measured from 0 in number of lattice cites) L_i in the i'th direction, we assume

$$\Psi(\mathbf{r} + L_i \mathbf{a}_i) = \Psi(\mathbf{r}) \tag{A.1}$$

We have symmetry breaking $\mathbb{Z}^d \to \otimes_i \mathbb{Z}_{L_i}$, meaning the solutions have reduced symmetry of $G = \otimes_i \mathbb{Z}_{L_i}$ instead of $\mathbb{Z}^d$. Justification is that for macroscopic lattices $L_i \sim O(10^{23})$, so it is a good approximation of infinite translation group. On the fig. A.1 we can see that the N'th roots of unity spaced by the angle $2\pi/N$ approximate the whole $U(1)$, which is parameterized by a continuous angle θ.

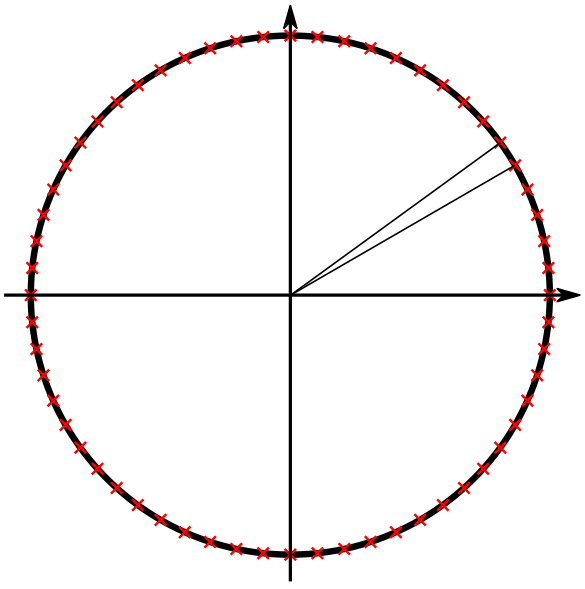

Figure A.1: Graphical representation of $U(1)$ and Z_N with $N = 60$

Now consider only translation in direction i. There is no group structure in $\mathbf{a}_i$ so we can write $T(n_i\mathbf{a}_i) \equiv T(n_i)$. This is a representation of

$$\mathbb{Z}_{L_i} \cong \langle g | g^{L_i} = e \rangle \tag{A.2}$$

a cyclic group of order L_i. It's reps. are characterized by $m_i \in \mathbb{Z}$, namely

$$D^{m_i}(g^{n_i}) = e^{i2\pi m_i n_i / L_i} \equiv e^{ik_i n_i} \tag{A.3}$$

with

$$k_i = 2\pi m_i / L_i \tag{A.4}$$

APPENDIX B

Tight Binding

Some explicit calculations for the tight binding model in the first quantization.

$$H_{AA} = \frac{1}{N}\sum_{\mathbf{R}_A\mathbf{R}'_A} e^{i\mathbf{k}\cdot(\mathbf{R}'_A-\mathbf{R}_A)}\langle\phi(\mathbf{r}-\mathbf{R}_A)|H_{\text{lattice}}|\phi(\mathbf{r}-\mathbf{R}'_A)\rangle \tag{B.1}$$

$$= \frac{1}{N}\sum_{\mathbf{R}_A\mathbf{R}'_A} e^{i\mathbf{k}\cdot(\mathbf{R}'_A-\mathbf{R}_A)}\langle\phi(\mathbf{r})|H_{\text{lattice}}|\phi(\mathbf{r}+\mathbf{R}_A-\mathbf{R}'_A)\rangle \tag{B.2}$$

$$= \frac{1}{N}\sum_{\mathbf{R}_A\mathbf{R}'_A} e^{i\mathbf{k}\cdot(\mathbf{R}'_A-\mathbf{R}_A)}\langle\phi(\mathbf{r})|H_{\text{lattice}}|\phi(\mathbf{r}+\mathbf{R}_A-\mathbf{R}'_A)\rangle \tag{B.3}$$

$$= \frac{1}{N}\sum_{\mathbf{R}_A\mathbf{d}} e^{i\mathbf{k}\cdot\mathbf{d}}\langle\phi(\mathbf{r})|H_{\text{lattice}}|\phi(\mathbf{r}-\mathbf{d})\rangle \tag{B.4}$$

$$= \sum_{\mathbf{d}} e^{i\mathbf{k}\cdot\mathbf{d}}\langle\phi(\mathbf{r})|H_{\text{lattice}}|\phi(\mathbf{r}-\mathbf{d})\rangle \tag{B.5}$$

$$H_{AB} = \frac{1}{N}\sum_{\mathbf{R}_A\mathbf{R}_B} e^{i\mathbf{k}\cdot(\mathbf{R}_B-\mathbf{R}_A)}\langle\phi(\mathbf{r}-\mathbf{R}_A)|H_{\text{lattice}}|\phi(\mathbf{r}-\mathbf{R}_B)\rangle \tag{B.6}$$

$$= \frac{1}{N}\sum_{\mathbf{R}_A\mathbf{R}_B} e^{i\mathbf{k}\cdot(\mathbf{R}_B-\mathbf{R}_A)}\langle\phi(\mathbf{r})|H_{\text{lattice}}|\phi(\mathbf{r}+\mathbf{R}_A-\mathbf{R}_B)\rangle \tag{B.7}$$

$$= \frac{1}{N}\sum_{\mathbf{R}_A\mathbf{R}_B} e^{i\mathbf{k}\cdot(\mathbf{R}_B-\mathbf{R}_A)}\langle\phi(\mathbf{r})|H_{\text{lattice}}|\phi(\mathbf{r}+\mathbf{R}_A-\mathbf{R}_B)\rangle \tag{B.8}$$

$$= \frac{1}{N}\sum_{\mathbf{R}_A\mathbf{d}} e^{i\mathbf{k}\cdot\mathbf{d}}\langle\phi(\mathbf{r})|H_{\text{lattice}}|\phi(\mathbf{r}-\mathbf{d})\rangle \tag{B.9}$$

$$= \sum_{\mathbf{d}} e^{i\mathbf{k}\cdot\mathbf{d}}\langle\phi(\mathbf{r})|H_{\text{lattice}}|\phi(\mathbf{r}-\mathbf{d})\rangle \tag{B.10}$$

$$S_{AA} = \frac{1}{N} \sum_{\mathbf{R}_A \mathbf{R}'_A} e^{i\mathbf{k}\cdot(\mathbf{R}'_A - \mathbf{R}_A)} \langle \phi(\mathbf{r} - \mathbf{R}_A) | \phi(\mathbf{r} - \mathbf{R}'_A) \rangle \tag{B.11}$$

$$= \frac{1}{N} \sum_{\mathbf{R}_A \mathbf{R}'_A} e^{i\mathbf{k}\cdot(\mathbf{R}'_A - \mathbf{R}_A)} \langle \phi(\mathbf{r}) | \phi(\mathbf{r} + \mathbf{R}_A - \mathbf{R}'_A) \rangle \tag{B.12}$$

$$= \frac{1}{N} \sum_{\mathbf{R}_A \mathbf{R}'_A} e^{i\mathbf{k}\cdot(\mathbf{R}'_A - \mathbf{R}_A)} \langle \phi(\mathbf{r}) | \phi(\mathbf{r} + \mathbf{R}_A - \mathbf{R}'_A) \rangle \tag{B.13}$$

$$= \frac{1}{N} \sum_{\mathbf{R}_A \mathbf{d}} e^{i\mathbf{k}\cdot\mathbf{d}} \langle \phi(\mathbf{r}) | \phi(\mathbf{r} - \mathbf{d}) \rangle \tag{B.14}$$

$$= \sum_{\mathbf{d}} e^{i\mathbf{k}\cdot\mathbf{d}} \langle \phi(\mathbf{r}) | \phi(\mathbf{r} - \mathbf{d}) \rangle \tag{B.15}$$

$$S_{AB} = \frac{1}{N} \sum_{\mathbf{R}_A \mathbf{R}_B} e^{i\mathbf{k}\cdot(\mathbf{R}_B - \mathbf{R}_A)} \langle \phi(\mathbf{r} - \mathbf{R}_A) | \phi(\mathbf{r} - \mathbf{R}_B) \rangle \tag{B.16}$$

$$= \frac{1}{N} \sum_{\mathbf{R}_A \mathbf{R}_B} e^{i\mathbf{k}\cdot(\mathbf{R}_B - \mathbf{R}_A)} \langle \phi(\mathbf{r}) | \phi(\mathbf{r} + \mathbf{R}_A - \mathbf{R}_B) \rangle \tag{B.17}$$

$$= \frac{1}{N} \sum_{\mathbf{R}_A \mathbf{R}_B} e^{i\mathbf{k}\cdot(\mathbf{R}_B - \mathbf{R}_A)} \langle \phi(\mathbf{r}) | \phi(\mathbf{r} + \mathbf{R}_A - \mathbf{R}_B) \rangle \tag{B.18}$$

$$= \frac{1}{N} \sum_{\mathbf{R}_A \mathbf{d}} e^{i\mathbf{k}\cdot\mathbf{d}} \langle \phi(\mathbf{r}) | \phi(\mathbf{r} - \mathbf{d}) \rangle \tag{B.19}$$

$$= \sum_{\mathbf{d}} e^{i\mathbf{k}\cdot\mathbf{d}} \langle \phi(\mathbf{r}) | \phi(\mathbf{r} - \mathbf{d}) \rangle \tag{B.20}$$

APPENDIX C

Operator properties

C.1 Operators

These hold in both x and y spin basis, i.e. $\uparrow\downarrow$ or $\leftrightarrows$

$$\begin{aligned}
&\{c_{l\sigma}, c_{ks}\} = 0 && \{c^\dagger_{l\sigma}, c^\dagger_{ks}\} = 0 && \{c_{l\sigma}, c^\dagger_{ks}\} = \delta_{lk}\delta_{\sigma s} \\
&\{\eta_{l\sigma}, \eta_{ks}\} = \frac{1}{2}\delta_{lk}\delta_{\sigma s} && \{\beta_{l\sigma}, \beta_{ks}\} = \frac{1}{2}\delta_{lk}\delta_{\sigma s} && \{\eta_{l\sigma}, \beta_{ks}\} = 0 \\
&\{d_{l\sigma}, d^\dagger_{ks}\} = \delta_{lk}\delta_{\sigma s} && \{d_{l\sigma}, d_{ks}\} = 0 && \{d^\dagger_{l\sigma}, d^\dagger_{ks}\} = 0
\end{aligned} \tag{C.1}$$

$$c^2_{l\sigma} = (c^\dagger_{l\sigma})^2 = d^2_{l\sigma} = (d^\dagger_{l\sigma})^2 = 0 \qquad \eta^2_{l\sigma} = \beta^2_{l\sigma} = \frac{1}{4} \tag{C.2}$$

C.2 Commutator identities

$$[AB, C] = [A, C]B + A[B, C] \tag{C.3}$$
$$[A, BC] = [A, B]C + B[A, C] \tag{C.4}$$
$$[AB, C] = \{A, C\}B - A\{B, C\} \tag{C.5}$$
$$[A, BC] = \{A, B\}C - B\{A, C\} \tag{C.6}$$

C.3 Majoranas on a hexagonal lattice

Kinetic term

$$\begin{aligned}
t c^\dagger_{i\sigma} c_{j\sigma} + h.c. &= t(\eta_{i\sigma} - i\beta_{i\sigma})(\beta_{j\sigma} + i\eta_{j\sigma}) + h.c. \\
&= 2it\eta_{i\sigma}\eta_{j\sigma} - 2it\beta_{i\sigma}\beta_{j\sigma}
\end{aligned}$$

Supeconductive pairing term

$$\begin{aligned}\Delta c^{\dagger}_{i\sigma} c^{\dagger}_{j\sigma} + h.c. &= \Delta(\eta_{i\sigma} - i\beta_{i\sigma})(\beta_{j\sigma} - i\eta_{j\sigma}) + h.c. \\ &= -2i\Delta\eta_{i\sigma}\eta_{j\sigma} - 2i\Delta\beta_{i\sigma}\beta_{j\sigma}\end{aligned}$$

Hubbard interaction term

$$\begin{aligned}\left(n_{i\uparrow} - \frac{1}{2}\right)\left(n_{i\downarrow} - \frac{1}{2}\right) &= \left((\eta_{i\uparrow} - i\beta_{i\uparrow})(\eta_{i\uparrow} + i\beta_{i\uparrow}) - \frac{1}{2}\right)\left((\eta_{i\downarrow} - i\beta_{i\downarrow})(\eta_{i\downarrow} + i\beta_{i\downarrow}) - \frac{1}{2}\right) \\ &= \left(-2i\beta_{i\uparrow}\eta_{i\uparrow} + \eta^2_{i\uparrow} + \beta^2_{i\uparrow} - \frac{1}{2}\right)\left(-2i\beta_{i\downarrow}\eta_{i\downarrow} + \eta^2_{i\downarrow} - i\beta^2_{i\downarrow} - \frac{1}{2}\right) \\ &= (-2i\beta_{i\uparrow}\eta_{i\uparrow})(-2i\beta_{i\downarrow}\eta_{i\downarrow})\end{aligned}$$

$$\begin{aligned}\left(n_{j\uparrow} - \frac{1}{2}\right)\left(n_{j\downarrow} - \frac{1}{2}\right) &= \left((\beta_{j\uparrow} - i\eta_{j\uparrow})(\beta_{j\uparrow} + i\eta_{j\uparrow}) - \frac{1}{2}\right)\left((\beta_{j\downarrow} - i\eta_{j\downarrow})(\beta_{j\downarrow} + i\eta_{j\downarrow}) - \frac{1}{2}\right) \\ &= \left(2i\beta_{j\uparrow}\eta_{j\uparrow} + \eta^2_{j\uparrow} + \beta^2_{j\uparrow} - \frac{1}{2}\right)\left(2i\beta_{j\downarrow}\eta_{j\downarrow} + \eta^2_{j\downarrow} - i\beta^2_{j\downarrow} - \frac{1}{2}\right) \\ &= (2i\beta_{j\uparrow}\eta_{j\uparrow})(2i\beta_{j\downarrow}\eta_{j\downarrow})\end{aligned}$$

C.4 Basis transformations

$\hat{z}$-spin ↔ $\hat{y}$-spin

Since eigenvalues of σ_z correspond to states polarized along the $\hat{z}$-axis (commonly referred to as up ↑ and down ↓) and they can be represented in the basis of eigenvectors of σ_y which represent $\hat{y}$-polarized spins (here left← and right→)

$$\sigma_z|\uparrow\rangle = |\uparrow\rangle \qquad \sigma_z|\downarrow\rangle = -|\downarrow\rangle \tag{C.7}$$

$$\sigma_y|\rightarrow\rangle = |\rightarrow\rangle \qquad \sigma_y|\leftarrow\rangle = -|\leftarrow\rangle \tag{C.8}$$

Using the eigenvectors of σ_y and σ_z Pauli matrices one can derive the following relations

$$|\leftarrow\rangle = \frac{1}{\sqrt{2}}(|\uparrow\rangle - i|\downarrow\rangle) \tag{C.9}$$

$$|\rightarrow\rangle = \frac{1}{\sqrt{2}}(|\uparrow\rangle + i|\downarrow\rangle) \tag{C.10}$$

c-fermion ↔ Majorana

$$\begin{aligned} c_{i\sigma} &= \eta_{i\sigma} + i\beta_{i\sigma} & c_{j\sigma} &= \beta_{j\sigma} + i\eta_{j\sigma} \\ \eta_{i\sigma} &= \frac{1}{2}(c_{i\sigma} + c_{i\sigma}^\dagger) & \beta_{i\sigma} &= \frac{1}{2i}(c_{i\sigma} - c_{i\sigma}^\dagger) \\ \eta_{j\sigma} &= \frac{1}{2i}(c_{j\sigma} - c_{j\sigma}^\dagger) & \beta_{j\sigma} &= \frac{1}{2}(c_{j\sigma} + c_{j\sigma}^\dagger) \end{aligned} \tag{C.11}$$

d-fermion ↔ Majorana

$$\begin{aligned} d_{i1} &= \beta_{i\uparrow} - i\beta_{i\downarrow} & d_{j1} &= \beta_{j\uparrow} + i\beta_{j\downarrow} & d_{i2} &= \eta_{i\uparrow} + i\eta_{i\downarrow} & d_{j2} &= \eta_{j\uparrow} - i\eta_{j\downarrow} \\ \beta_{i\uparrow} &= \frac{1}{2}(d_{i1} + d_{i1}^\dagger) & \beta_{j\uparrow} &= \frac{1}{2}(d_{j1} + d_{j1}^\dagger) & \eta_{i\uparrow} &= \frac{1}{2}(d_{i2} + d_{i2}^\dagger) & \eta_{j\uparrow} &= \frac{1}{2}(d_{j2} + d_{j2}^\dagger) \\ \beta_{i\downarrow} &= \frac{1}{2i}(d_{i1}^\dagger - d_{i1}) & \beta_{j\downarrow} &= \frac{1}{2}(d_{j1} - d_{j1}^\dagger) & \eta_{i\downarrow} &= \frac{1}{2}(d_{i2} - d_{i2}^\dagger) & \eta_{j\downarrow} &= \frac{1}{2}(d_{j2}^\dagger - d_{j2}) \end{aligned} \tag{C.12}$$

Calculating Hamiltonian

$$\begin{aligned} 4\beta_{i\uparrow}\beta_{j\uparrow} + 4\beta_{i\downarrow}\beta_{j\downarrow} &= (d_{i1} + d_{i1}^\dagger)(d_{j1} + d_{j1}^\dagger) + (d_{i1} - d_{i1}^\dagger)(d_{j1} - d_{j1}^\dagger) \\ &= d_{i1}d_{j1} + d_{i1}^\dagger d_{j1}^\dagger + d_{i1}d_{j1}^\dagger + d_{i1}^\dagger d_{j1} + d_{i1}d_{j1} + d_{i1}^\dagger d_{j1}^\dagger - d_{i1}d_{j1}^\dagger - d_{i1}^\dagger d_{j1} \\ &= 2d_{i1}d_{j1} + 2d_{i1}^\dagger d_{j1}^\dagger \end{aligned}$$

$$\begin{aligned} 4\eta_{i\uparrow}\eta_{j\uparrow} + 4\eta_{i\downarrow}\eta_{j\downarrow} &= (d_{i2} + d_{i2}^\dagger)(d_{j2} + d_{j2}^\dagger) + (d_{i2} - d_{i2}^\dagger)(d_{j2} - d_{j2}^\dagger) \\ &= d_{i2}d_{j2} + d_{i2}^\dagger d_{j2}^\dagger + d_{i2}d_{j2}^\dagger + d_{i2}^\dagger d_{j2} + d_{i2}d_{j2} + d_{i2}^\dagger d_{j2}^\dagger - d_{i2}d_{j2}^\dagger - d_{i2}^\dagger d_{j2} \\ &= 2d_{i2}d_{j2} + 2d_{i2}^\dagger d_{j2}^\dagger \end{aligned}$$

$$\begin{aligned} (2i\beta_{i\uparrow}\beta_{i\downarrow})(2i\eta_{i\uparrow}\eta_{i\downarrow}) &= \frac{1}{4}(d_{i1} + d_{i1}^\dagger)(d_{i1}^\dagger - d_{i1})(d_{i2} + d_{i2}^\dagger)(d_{i2} - d_{i2}^\dagger) \\ &= \frac{1}{4}(d_{i1}d_{i1}^\dagger - d_{i1}^\dagger d_{i1})(-d_{i2}d_{i2}^\dagger + d_{i2}^\dagger d_{i2}) \\ &= \frac{1}{4}(1 - 2d_{i1}^\dagger d_{i1})(-1 + 2d_{i2}^\dagger d_{i2}) \\ &= -\left(n_{i1} - \frac{1}{2}\right)\left(n_{i2} - \frac{1}{2}\right) \end{aligned}$$

$$
\begin{aligned}
(2i\beta_{j\uparrow}\beta_{j\downarrow})(2i\eta_{j\uparrow}\eta_{j\downarrow}) &= \frac{1}{4}(d_{j1}+d_{j1}^\dagger)(d_{j1}-d_{j1}^\dagger)(d_{j2}+d_{j2}^\dagger)(d_{j2}^\dagger-d_{j2}) \\
&= \frac{1}{4}(d_{j1}^\dagger d_{j1}-d_{j1}d_{j1}^\dagger)(d_{j2}d_{j2}^\dagger-d_{j2}^\dagger d_{j2}) \\
&= \frac{1}{4}(2d_{j1}^\dagger d_{j1}-1)(1-2d_{j2}^\dagger d_{j2}) \\
&= -\left(n_{j1}-\frac{1}{2}\right)\left(n_{j2}-\frac{1}{2}\right)
\end{aligned}
$$

d-fermion ↔ *c*-fermion

For completeness we write out the explicit transformation from c to d fermions.

$$
\begin{aligned}
d_{i1} &= \beta_{i\uparrow}-i\beta_{i\downarrow} \\
&= \frac{1}{2i}(c_{i\uparrow}-c_{i\uparrow}^\dagger)-i\frac{1}{2i}(c_{i\downarrow}-c_{i\downarrow}^\dagger) \\
&= \frac{1}{i\sqrt{2}}\left[\frac{1}{\sqrt{2}}(c_{i\uparrow}-ic_{i\downarrow})-\frac{1}{\sqrt{2}}(c_{i\uparrow}+ic_{i\downarrow})^\dagger\right] \\
&= \frac{1}{i\sqrt{2}}(c_{i\leftarrow}-c_{i\rightarrow}^\dagger)
\end{aligned}
$$

$$
\begin{aligned}
d_{i2} &= \eta_{i\uparrow}+i\eta_{i\downarrow} \\
&= \frac{1}{2}(c_{i\uparrow}+c_{i\uparrow}^\dagger)+i\frac{1}{2}(c_{i\downarrow}+c_{i\downarrow}^\dagger) \\
&= \frac{1}{\sqrt{2}}\left[\frac{1}{\sqrt{2}}(c_{i\uparrow}+ic_{i\downarrow})+\frac{1}{\sqrt{2}}(c_{i\uparrow}-ic_{i\downarrow})^\dagger\right] \\
&= \frac{1}{\sqrt{2}}(c_{i\rightarrow}+c_{i\leftarrow}^\dagger)
\end{aligned}
$$

$$
\begin{aligned}
d_{j1} &= \beta_{j\uparrow}+i\beta_{j\downarrow} \\
&= \frac{1}{2}(c_{j\uparrow}+c_{j\uparrow}^\dagger)+i\frac{1}{2}(c_{j\downarrow}+c_{j\downarrow}^\dagger) \\
&= \frac{1}{\sqrt{2}}\left[\frac{1}{\sqrt{2}}(c_{j\uparrow}+ic_{j\downarrow})+\frac{1}{\sqrt{2}}(c_{j\uparrow}-ic_{j\downarrow})^\dagger\right] \\
&= \frac{1}{\sqrt{2}}(c_{j\rightarrow}+c_{j\leftarrow}^\dagger)
\end{aligned}
$$

$$
\begin{aligned}
d_{j2} &= \eta_{j\uparrow}-i\eta_{j\downarrow} \\
&= \frac{1}{2i}(c_{j\uparrow}-c_{j\uparrow}^\dagger)-i\frac{1}{2i}(c_{j\downarrow}-c_{j\downarrow}^\dagger) \\
&= \frac{1}{i\sqrt{2}}\left[\frac{1}{\sqrt{2}}(c_{j\uparrow}-ic_{j\downarrow})-\frac{1}{\sqrt{2}}(c_{j\uparrow}+ic_{j\downarrow})^\dagger\right]
\end{aligned}
$$

$$= \frac{1}{i\sqrt{2}}(c_{j\leftarrow} - c^\dagger_{j\rightarrow})$$

C.5 d-fermion eigenstates

$$\begin{aligned}
|\rightarrow\rangle_d = d^\dagger_\rightarrow|0\rangle_d &= \frac{1}{\sqrt{2}}(c^\dagger_\rightarrow + c_\leftarrow)\frac{1}{\sqrt{2}}(1 + c^\dagger_\leftarrow c^\dagger_\rightarrow)|0\rangle \\
&= \frac{1}{2}(c^\dagger_\rightarrow + c_\leftarrow c^\dagger_\leftarrow c^\dagger_\rightarrow)|0\rangle \\
&= \frac{1}{2}(c^\dagger_\rightarrow + \{c_\leftarrow, c^\dagger_\leftarrow\}c^\dagger_\rightarrow)|0\rangle \\
&= c^\dagger_\rightarrow|0\rangle
\end{aligned}$$

$$\begin{aligned}
|\leftarrow\rangle_d = d^\dagger_\leftarrow|0\rangle_d &= \frac{1}{i\sqrt{2}}(c_\rightarrow - c^\dagger_\leftarrow)\frac{1}{\sqrt{2}}(1 + c^\dagger_\leftarrow c^\dagger_\rightarrow)|0\rangle \\
&= \frac{i}{2}(c^\dagger_\leftarrow - c_\rightarrow c^\dagger_\leftarrow c^\dagger_\rightarrow)|0\rangle \\
&= \frac{1}{2}(c^\dagger_\rightarrow + c^\dagger_\leftarrow\{c_\rightarrow, c^\dagger_\rightarrow\})|0\rangle \\
&= ic^\dagger_\leftarrow|0\rangle
\end{aligned}$$

$$\begin{aligned}
|\leftrightarrows\rangle_d = d^\dagger_\leftarrow d^\dagger_\rightarrow|0\rangle_d &= \frac{1}{i\sqrt{2}}(c_\rightarrow - c^\dagger_\leftarrow)c^\dagger_\rightarrow|0\rangle \\
&= \frac{1}{i\sqrt{2}}(c_\rightarrow c^\dagger_\rightarrow - c^\dagger_\leftarrow c^\dagger_\rightarrow)|0\rangle \\
&= \frac{1}{i\sqrt{2}}(\{c_\rightarrow, c^\dagger_\rightarrow\} - c^\dagger_\leftarrow c^\dagger_\rightarrow)|0\rangle \\
&= \frac{-i}{\sqrt{2}}(1 - c^\dagger_\leftarrow c^\dagger_\rightarrow)|0\rangle
\end{aligned}$$

Orthonormality

$$\begin{aligned}
{}_d\langle 0|0\rangle_d &= \langle 0|\frac{1}{\sqrt{2}}(1 + c_\rightarrow c_\leftarrow)\frac{1}{\sqrt{2}}(1 + c^\dagger_\leftarrow c^\dagger_\rightarrow)|0\rangle \\
&= \frac{1}{2}\langle 0|1 + c_\rightarrow c_\leftarrow + c^\dagger_\leftarrow c^\dagger_\rightarrow + c_\rightarrow c_\leftarrow c^\dagger_\leftarrow c^\dagger_\rightarrow|0\rangle \\
&= \frac{1}{2}\langle 0|1 + 0 + 0 + 1|0\rangle \\
&= 1
\end{aligned}$$

$$
\begin{aligned}
{}_d\langle \rightarrow |0\rangle_d &= \langle 0|c_\rightarrow \frac{1}{\sqrt{2}}(1 + c^\dagger_\leftarrow c^\dagger_\rightarrow)|0\rangle \\
&= \frac{1}{\sqrt{2}}\langle 0|c_\rightarrow + c_\rightarrow c^\dagger_\leftarrow c^\dagger_\rightarrow|0\rangle \\
&= \frac{1}{\sqrt{2}}\langle 0|0 - 0|0\rangle \\
&= 0
\end{aligned}
$$

$$
\begin{aligned}
{}_d\langle \leftarrow |0\rangle_d &= \langle 0| - ic_\leftarrow \frac{1}{\sqrt{2}}(1 + c^\dagger_\leftarrow c^\dagger_\rightarrow)|0\rangle \\
&= -i\frac{1}{\sqrt{2}}\langle 0|c_\leftarrow + c_\leftarrow c^\dagger_\leftarrow c^\dagger_\rightarrow|0\rangle \\
&= -i\frac{1}{\sqrt{2}}\langle 0|0 + 0|0\rangle \\
&= 0
\end{aligned}
$$

$$
\begin{aligned}
{}_d\langle \leftrightarrows |0\rangle_d &= \langle 0|\frac{i}{\sqrt{2}}(1 - c_\rightarrow c_\leftarrow)\frac{1}{\sqrt{2}}(1 + c^\dagger_\leftarrow c^\dagger_\rightarrow)|0\rangle \\
&= \frac{i}{2}\langle 0|1 - c_\rightarrow c_\leftarrow + c^\dagger_\leftarrow c^\dagger_\rightarrow - c_\rightarrow c_\leftarrow c^\dagger_\leftarrow c^\dagger_\rightarrow|0\rangle \\
&= \frac{1}{2}\langle 0|1 - 0 + 0 - 1|0\rangle \\
&= 0
\end{aligned}
$$

D_l eigenvalues

$$
D_l|0\rangle_d = \begin{cases} -|0\rangle_d & l \in A \\ |0\rangle_d & l \in B \end{cases} \qquad \xi_l D_l|0\rangle_d = -|0\rangle_d
$$

$$
D_l|l \rightarrow\rangle_d = |l \rightarrow\rangle_d \qquad \xi_l D_l|l \rightarrow\rangle_d = \begin{cases} |l \rightarrow\rangle_d & l \in A \\ -|l \rightarrow\rangle_d & l \in B \end{cases}
$$

$$
D_l|l \leftarrow\rangle_d = -|l \leftarrow\rangle_d \qquad \xi_l D_l|l \leftarrow\rangle_d = \begin{cases} -|l \leftarrow\rangle_d & l \in A \\ |l \leftarrow\rangle_d & l \in B \end{cases}
$$

$$
D_l|l \leftrightarrows\rangle_d = \begin{cases} |l \leftrightarrows\rangle_d & l \in A \\ -|l \leftrightarrows\rangle_d & l \in B \end{cases} \qquad \xi_l D_l|l \leftrightarrows\rangle_d = |l \leftrightarrows\rangle_d
$$

APPENDIX D

Fourier transforms

D.1 ANR

Simplest are the ones contained in Hubbard interaction term

$$\sum_{lm} {d^{\lambda}}^{\dagger}_{lm} d^{\lambda}_{lm} = \frac{1}{L_y} \sum_{lmkk'} e^{i(-k+k')y_{lm\lambda}} {d^{\lambda}}^{\dagger}_{km} d^{\lambda}_{k'm} \tag{D.1}$$

$$= \sum_{mkk'} \delta_{k,k'} {d^{\lambda}}^{\dagger}_{km} d^{\lambda}_{k'm} \tag{D.2}$$

$$= \sum_{mk} {d^{\lambda}}^{\dagger}_{km} d^{\lambda}_{km} \tag{D.3}$$

Next we go through the free Hamiltonian term-by-term

$$\sum_{l} \sum_{m\in\text{odd}} d^{a}_{lm} d^{b}_{l-1m} = \frac{1}{L_y} \sum_{lkk'} \sum_{m\in\text{odd}} e^{ik'y_{lma}} e^{iky_{l-1mb}} d^{a}_{k'm} d^{b}_{km} \tag{D.4}$$

$$= \frac{1}{L_y} \sum_{lkk'} \sum_{m\in\text{odd}} e^{ik'y_l} e^{ik(y_l-a)} d^{a}_{k'm} d^{b}_{km} \tag{D.5}$$

$$= \frac{1}{L_y} \sum_{lkk'} \sum_{m\in\text{odd}} e^{i(k'+k)y_l} e^{-ika} d^{a}_{k'm} d^{b}_{km} \tag{D.6}$$

$$= \sum_{kk'} \sum_{m\in\text{odd}} \delta_{k',-k} e^{-ika} d^{a}_{k'm} d^{b}_{km} \tag{D.7}$$

$$= \sum_{k} \sum_{m\in\text{odd}} e^{-ika} d^{a}_{-km} d^{b}_{km} \tag{D.8}$$

$$\tag{D.9}$$

$$\sum_{l} \sum_{m\in\text{even}} d^{a}_{lm} d^{b}_{lm} = \frac{1}{L_y} \sum_{lkk'} \sum_{m\in\text{even}} e^{ik'y_{lma}} e^{iky_{lmb}} d^{a}_{k'm} d^{b}_{km} \tag{D.10}$$

$$= \frac{1}{L_y} \sum_{lkk'} \sum_{m\in\text{even}} e^{ik'(y_l+a\cos(\pi/3)+a)} e^{ik(y_l+a\cos(\pi/3))} d^{a}_{k'm} d^{b}_{km} \tag{D.11}$$

$$= \frac{1}{L_y} \sum_{lkk'} \sum_{m\in\text{even}} e^{i(k'+k)y_l} e^{i(k'+k)a\cos(\pi/3)} e^{ik'a} d^a_{k'm} d^b_{km} \tag{D.12}$$

$$= \sum_{kk'} \sum_{m\in\text{even}} \delta_{k',-k} e^{i(k'+k)a\cos(\pi/3)} e^{ik'a} d^a_{k'm} d^b_{km} \tag{D.13}$$

$$= \sum_{k} \sum_{m\in\text{even}} e^{-ika} d^a_{-km} d^b_{km} \tag{D.14}$$

$$\sum_l \sum_{m\in\text{odd}} d^a_{lm+1} d^b_{lm} = \frac{1}{L_y} \sum_{lkk'} \sum_{m\in\text{odd}} e^{ik'(y_l+a\cos(\pi/3)+a)} e^{ik(y_l+2a)} d^a_{k'm+1} d^b_{km} \tag{D.15}$$

$$= \sum_{kk'} \sum_{m\in\text{odd}} \delta_{k',-k} e^{ik'(a\cos(\pi/3)+a)} e^{2ika} d^a_{k'm+1} d^b_{km} \tag{D.16}$$

$$= \sum_{k} \sum_{m\in\text{odd}} e^{-ik(a\cos(\pi/3)+a)} e^{2ika} d^a_{-km+1} d^b_{km} \tag{D.17}$$

$$= \sum_{k} \sum_{m=1}^{N-1} e^{ika/2} d^a_{-km+1} d^b_{km} \tag{D.18}$$

$$= \sum_{k} \sum_{m=1}^{N-1} e^{-ika} e^{ika_T/2} d^a_{-km+1} d^b_{km} \tag{D.19}$$

$$\sum_l \sum_{m\in\text{even}} d^a_{lm+1} d^b_{lm} = \frac{1}{L_y} \sum_{lkk'} \sum_{m\in\text{even}} e^{ik'y_l} e^{ik(y_l+a\cos(\pi/3))} d^a_{k'm+1} d^b_{km} \tag{D.20}$$

$$= \sum_{kk'} \sum_{m\in\text{even}} \delta_{k',-k} e^{ik(a\cos(\pi/3))} d^a_{k'm+1} d^b_{km} \tag{D.21}$$

$$= \sum_{k} \sum_{m\in\text{even}} e^{ik(a\cos(\pi/3))} d^a_{-km+1} d^b_{km} \tag{D.22}$$

$$= \sum_{k} \sum_{m=1}^{N-1} e^{ika/2} d^a_{-km+1} d^b_{km} \tag{D.23}$$

$$= \sum_{k} \sum_{m=1}^{N-1} e^{-ika} e^{ika_T/2} d^a_{-km+1} d^b_{km} \tag{D.24}$$

D.2 ZNR

$$d^a_{lm} = \frac{1}{\sqrt{L_y}} \sum_k e^{iky_{lma}} d^a_{km} \qquad d^b_{lm} = \frac{1}{\sqrt{L_y}} \sum_k e^{iky_{lmb}} d^b_{km} \tag{D.25}$$

$$\sum_l \sum_{m\in\text{even}} d^a_{lm} d^b_{l-1m} = \frac{1}{L_y} \sum_{lk'k} \sum_{m\in\text{even}} e^{ik'y_{lma}} e^{iky_{lmb} - ika\sqrt{3}} d^a_{k'm} d^b_{km} \tag{D.26}$$

$$= \frac{1}{L_y} \sum_{lk'k} \sum_{m\in\text{even}} e^{ik'y_l - ik'a\sqrt{3}/2} e^{iky_l - ika\sqrt{3}} d^a_{k'm} d^b_{km} \tag{D.27}$$

$$= \sum_{k'k} \sum_{m\in\text{even}} \delta_{k',-k} e^{-ik'a\sqrt{3}/2} e^{-ika\sqrt{3}} d^a_{k'm} d^b_{km} \tag{D.28}$$

$$= \sum_{k} \sum_{m\in\text{even}} e^{ika\sqrt{3}/2} e^{-ika\sqrt{3}} d^a_{-km} d^b_{km} \tag{D.29}$$

$$\sum_{l} \sum_{m\in\text{odd}} d^a_{l-1m} d^b_{lm} = \frac{1}{L_y} \sum_{lk'k} \sum_{m\in\text{odd}} e^{ik'y_{lma} - ik'a\sqrt{3}} e^{iky_{lmb}} d^a_{k'm} d^b_{km} \tag{D.30}$$

$$= \frac{1}{L_y} \sum_{lk'k} \sum_{m\in\text{odd}} e^{ik'y_l - ik'a\sqrt{3}} e^{iky_l - ika\sqrt{3}/2} d^a_{k'm} d^b_{km} \tag{D.31}$$

$$= \sum_{k'k} \sum_{m\in\text{odd}} \delta_{k',-k} e^{-ik'a\sqrt{3}} e^{-ika\sqrt{3}/2} d^a_{k'm} d^b_{km} \tag{D.32}$$

$$= \sum_{k} \sum_{m\in\text{odd}} e^{ika\sqrt{3}} e^{-ika\sqrt{3}/2} d^a_{-km} d^b_{km} \tag{D.33}$$

$$\sum_{l} \sum_{m\in\text{even}} d^a_{lm} d^b_{lm} = \frac{1}{L_y} \sum_{lk'k} \sum_{m\in\text{even}} e^{ik'y_{lma}} e^{iky_{lmb}} d^a_{k'm} d^b_{km} \tag{D.34}$$

$$= \frac{1}{L_y} \sum_{lk'k} \sum_{m\in\text{even}} e^{ik'y_l - ik'a\sqrt{3}/2} e^{iky_l} d^a_{k'm} d^b_{km} \tag{D.35}$$

$$= \sum_{k'k} \sum_{m\in\text{even}} \delta_{k',-k} e^{-ik'a\sqrt{3}/2} d^a_{k'm} d^b_{km} \tag{D.36}$$

$$= \sum_{k} \sum_{m\in\text{even}} e^{ika\sqrt{3}/2} d^a_{-km} d^b_{km} \tag{D.37}$$

$$\sum_{l} \sum_{m\in\text{odd}} d^a_{lm} d^b_{lm} = \frac{1}{L_y} \sum_{lk'k} \sum_{m\in\text{odd}} e^{ik'y_{lma}} e^{iky_{lmb}} d^a_{k'm} d^b_{km} \tag{D.38}$$

$$= \frac{1}{L_y} \sum_{lk'k} \sum_{m\in\text{odd}} e^{ik'y_l} e^{iky_l - ika\sqrt{3}/2} d^a_{k'm} d^b_{km} \tag{D.39}$$

$$= \sum_{k'k} \sum_{m\in\text{odd}} \delta_{k',-k} e^{-ika\sqrt{3}/2} d^a_{k'm} d^b_{km} \tag{D.40}$$

$$= \sum_{k} \sum_{m\in\text{odd}} e^{-ika\sqrt{3}/2} d^a_{-km} d^b_{km} \tag{D.41}$$

$$\sum_{l} \sum_{m\in\text{even}} d^a_{lm+1} d^b_{lm} = \frac{1}{L_y} \sum_{lk'k} \sum_{m\in\text{even}} e^{ik'y_{lma}} e^{iky_{lmb}} d^a_{k'm+1} d^b_{km} \tag{D.42}$$

$$= \frac{1}{L_y} \sum_{lk'k} \sum_{m\in\text{even}} e^{ik'y_l} e^{iky_l} d^a_{k'm+1} d^b_{km} \tag{D.43}$$

$$= \sum_{k'k} \sum_{m\in\text{even}} \delta_{k',-k} d^a_{k'm+1} d^b_{km} \tag{D.44}$$

$$= \sum_{k} \sum_{m\in\text{even}} d^a_{-km+1} d^b_{km} \tag{D.45}$$

$$\sum_{l} \sum_{m\in\text{odd}} d^a_{lm+1} d^b_{lm} = \frac{1}{L_y} \sum_{lk'k} \sum_{m\in\text{odd}} e^{ik'y_{lma}} e^{iky_{lmb}} d^a_{k'm+1} d^b_{km} \tag{D.46}$$

$$= \frac{1}{L_y} \sum_{lk'k} \sum_{m\in\text{odd}} e^{ik'y_l - ik'a\sqrt{3}/2} e^{iky_l - ika\sqrt{3}/2} d^a_{k'm+1} d^b_{km} \tag{D.47}$$

$$= \sum_{k'k} \sum_{m\in\text{odd}} \delta_{k',-k} e^{-ik'a\sqrt{3}/2} e^{-ika\sqrt{3}/2} d^a_{k'm+1} d^b_{km} \tag{D.48}$$

$$= \sum_{k} \sum_{m\in\text{odd}} d^a_{-km+1} d^b_{km} \tag{D.49}$$

Bibliography

[1] N. Ashcroft and N. Mermin, *Solid State Physics*, HRW international editions, Holt, Rinehart and Winston, 1976, ISBN: 9780030839931 (cit. on p. 3).

[2] L. Landau and E. Lifshitz, *Quantum Mechanics*, Course of Theoretical Physics, Pergamon Press, 1977, ISBN: 0080291406 (cit. on p. 3).

[3] W. Nolting, *Quantenmechanik*, Grundkurs: Theoretische Physik, Zimmermann-Neufang, 1993, ISBN: 3922410278 (cit. on p. 3).

[4] H. Georgi, *Lie algebras in particle physics*, 2nd ed., Perseus Books, 1999 (cit. on p. 3).

[5] *Undecidability of the spectral gap*, Nature **528** (7581 2015) 207, URL: https://doi.org/10.1038/nature16059 (cit. on p. 3).

[6] F. Bloch, *Über die Quantenmechanik der Elektronen in Kristallgittern*, Zeitschrift für Physik **52** (7 1929) 555 (cit. on p. 5).

[7] H. Bethe, *Termaufspaltung in Kristallen*, Annalen der Physik **395** (1929) 133, eprint: https://onlinelibrary.wiley.com/doi/pdf/10.1002/andp.19293950202, URL: https://onlinelibrary.wiley.com/doi/abs/10.1002/andp.19293950202 (cit. on p. 6).

[8] A. Akhmerov, *Online course on topology in condensed matter*, URL: https://topocondmat.org/ (cit. on p. 11).

[9] S. Shen, *Topological Insulators*, Springer Series in Solid-State Sciences, Springer-Verlag Berlin Heidelberg, 2012, ISBN: 9783642328589 (cit. on p. 11).

[10] J. McGreevy, *Topology from Physics*, 2021, URL: https://mcgreevy.physics.ucsd.edu/w21 (cit. on p. 11).

[11] A. Y. Kitaev, *Unpaired Majorana fermions in quantum wires*, Uspekhi Fizicheskikh Nauk (UFN) **44** (2001) 131, URL: https://doi.org/10.1070/1063-7869/44/10s/s29 (cit. on pp. 11, 12).

[12] J. K. Asbóth, L. Oroszlány and A. Pályi, *A Short Course on Topological Insulators*, Lecture Notes in Physics (2016), ISSN: 1616-6361, URL: http://dx.doi.org/10.1007/978-3-319-25607-8 (cit. on p. 11).

[13] K. v. Klitzing, G. Dorda and M. Pepper, *New Method for High-Accuracy Determination of the Fine-Structure Constant Based on Quantized Hall Resistance*, Phys. Rev. Lett. **45** (6 1980) 494, URL: https://link.aps.org/doi/10.1103/PhysRevLett.45.494 (cit. on p. 11).

[14] J. Zhu, *Bogoliubov-de Gennes Method and Its Applications*, English, vol. 924, Lecture Notes in Physics, Springer International Publishing, 2016, ISBN: 9783319313146 (cit. on p. 16).

[15] W. P. Su, J. R. Schrieffer and A. J. Heeger, *Soliton excitations in polyacetylene*, Phys. Rev. B **22** (4 1980) 2099, URL: https://link.aps.org/doi/10.1103/PhysRevB.22.2099 (cit. on p. 16).

[16] Z. Chen, X. Li and T. K. Ng, *Exactly Solvable BCS-Hubbard Model in Arbitrary Dimensions*, Phys. Rev. Lett. **120** (4 2018) 046401, URL: https://link.aps.org/doi/10.1103/PhysRevLett.120.046401 (cit. on p. 21).

[17] M. Ezawa, *Exact solutions for two-dimensional topological superconductors: Hubbard interaction induced spontaneous symmetry breaking*, Phys. Rev. B **97** (24 2018) 241113, URL: https://link.aps.org/doi/10.1103/PhysRevB.97.241113 (cit. on pp. 21, 30).

[18] J.-J. Miao, D.-H. Xu, L. Zhang and F.-C. Zhang, *Exact solution to the Haldane-BCS-Hubbard model along the symmetric lines: Interaction-induced topological phase transition*, Phys. Rev. B **99** (24 2019) 245154, URL: https://link.aps.org/doi/10.1103/PhysRevB.99.245154 (cit. on pp. 21, 30).

[19] A. Kitaev, *Anyons in an exactly solved model and beyond*, Annals of Physics **321** (2006) 2, ISSN: 0003-4916, URL: http://dx.doi.org/10.1016/j.aop.2005.10.005 (cit. on p. 21).

[20] K. Wakabayashi, K. Sasaki, T. Nakanishi and T. Enoki, *Electronic states of graphene nanoribbons and analytical solutions*, Science and Technology of Advanced Materials **11** (2010) 054504, URL: https://doi.org/10.1088/1468-6996/11/5/054504 (cit. on p. 32).

[21] C. L. Kane and E. J. Mele, *Z2Topological Order and the Quantum Spin Hall Effect*, Physical Review Letters **95** (2005), ISSN: 1079-7114, URL: http://dx.doi.org/10.1103/PhysRevLett.95.146802 (cit. on p. 38).

List of Figures